Rangeland Ecol Manage 63:16–39 | January 2010 | DOI: 10.2111/REM-D-09-00072.1

Productivity, Respiration, and Light-Response Parameters of World Grassland and Agroecosystems Derived From Flux-Tower Measurements

Tagir G. Gilmanov,[1] L. Aires,[2] Z. Barcza,[2] V. S. Baron,[3] L. Belelli,[2] J. Beringer,[2] D. Billesbach,[3] D. Bonal,[2] J. Bradford,[2] E. Ceschia,[2] D. Cook,[2] C. Corradi,[2] A. Frank,[4] D. Gianelle,[2] C. Gimeno,[2,3] T. Gruenwald,[2] Haiqiang Guo,[2] N. Hanan,[2] L. Haszpra,[2] J. Heilman,[2,3] A. Jacobs,[2] M. B. Jones,[3] D. A. Johnson,[4] G. Kiely,[2] Shenggong Li,[2] V. Magliulo,[2] E. Moors,[2] Z. Nagy,[2,3] M. Nasyrov,[3] C. Owensby,[3] K. Pinter,[2,3] C. Pio,[2] M. Reichstein,[2] M. J. Sanz,[2,3] R. Scott,[2] J. F. Soussana,[2,3] P. C. Stoy,[2] T. Svejcar,[4] Z. Tuba,[2,3,5] and Guangsheng Zhou[2]

Authors are [1]Professor, Department of Biology and Microbiology, South Dakota State University, Brookings, SAG 304, Box 2207B, SD 57007, USA; and researchers who contributed their data to the [2]FLUXNET La Thuile data set, [3]WORLDGRASSAGRIFLUX data set, or [4]US Department of Agriculture–Agricultural Research Service RANGEFLUX data set. [5]Deceased.

Abstract

Grasslands and agroecosystems occupy one-third of the terrestrial area, but their contribution to the global carbon cycle remains uncertain. We used a set of 316 site-years of CO_2 exchange measurements to quantify gross primary productivity, respiration, and light-response parameters of grasslands, shrublands/savanna, wetlands, and cropland ecosystems worldwide. We analyzed data from 72 global flux-tower sites partitioned into gross photosynthesis and ecosystem respiration with the use of the light-response method (Gilmanov, T. G., D. A. Johnson, and N. Z. Saliendra. 2003. Growing season CO_2 fluxes in a sagebrush-steppe ecosystem in Idaho: Bowen ratio/energy balance measurements and modeling. *Basic and Applied Ecology* 4:167–183) from the RANGEFLUX and WORLDGRASSAGRIFLUX data sets supplemented by 46 sites from the FLUXNET La Thuile data set partitioned with the use of the temperature-response method (Reichstein, M., E. Falge, D. Baldocchi, D. Papale, R. Valentini, M. Aubinet, P. Berbigier, C. Bernhofer, N. Buchmann, M. Falk, T. Gilmanov, A. Granier, T. Grünwald, K. Havránková, D. Janous, A. Knohl, T. Laurela, A. Lohila, D. Loustau, G. Matteucci, T. Meyers, F. Miglietta, J. M. Ourcival, D. Perrin, J. Pumpanen, S. Rambal, E. Rotenberg, M. Sanz, J. Tenhunen, G. Seufert, F. Vaccari, T. Vesala, and D. Yakir. 2005. On the separation of net ecosystem exchange into assimilation and ecosystem respiration: review and improved algorithm. *Global Change Biology* 11:1424–1439). Maximum values of the quantum yield ($\alpha = 75$ mmol $\cdot$ mol^{-1}), photosynthetic capacity ($A_{max} = 3.4$ mg $CO_2 \cdot m^{-2} \cdot s^{-1}$), gross photosynthesis ($P_{g,max} = 116$ g $CO_2 \cdot m^{-2} \cdot d^{-1}$), and ecological light-use efficiency ($\varepsilon_{ecol} = 59$ mmol $\cdot$ mol^{-1}) of managed grasslands and high-production croplands exceeded those of most forest ecosystems, indicating the potential of nonforest ecosystems for uptake of atmospheric CO_2. Maximum values of gross primary production (8 600 g $CO_2 \cdot m^{-2} \cdot yr^{-1}$), total ecosystem respiration (7 900 g $CO_2 \cdot m^{-2} \cdot yr^{-1}$), and net CO_2 exchange (2 400 g $CO_2 \cdot m^{-2} \cdot yr^{-1}$) were observed for intensively managed grasslands and high-yield crops, and are comparable to or higher than those for forest ecosystems, excluding some tropical forests. On average, 80% of the nonforest sites were apparent sinks for atmospheric CO_2, with mean net uptake of 700 g $CO_2 \cdot m^{-2} \cdot yr^{-1}$ for intensive grasslands and 933 g $CO_2 \cdot m^{-2} \cdot d^{-1}$ for croplands. However, part of these apparent sinks is accumulated in crops and forage, which are carbon pools that are harvested, transported, and decomposed off site. Therefore, although agricultural fields may be predominantly sinks for atmospheric CO_2, this does not imply that they are necessarily increasing their carbon stock.

Resumen

Los pastizales y agro-ecosistemas ocupan un tercio de la superficie terrestre, pero su contribución en el ciclo del carbono global sigue siendo desconocida. Utilizamos un conjunto de 316 sitios-años de mediciones de intercambio de CO_2 para cuantificar la productividad primaria bruta, respiración y parámetros de la a respuesta a la luz de pastizales, matorrales/sabana, humedales y los ecosistemas de tierras de cultivo en todo el mundo. Se analizaron datos de 72 torres en sitios de flujo global divididos en fotosíntesis bruta y respiración del ecosistema mediante el método de respuesta de luz (Gilmanov, T. G., D. A. Johnson, and N. Z. Saliendra. 2003. Growing season CO_2 fluxes in a sagebrush-steppe ecosystem in Idaho: Bowen ratio/energy balance measurements and modeling. *Basic and Applied Ecology* 4:167–183) de los conjuntos de datos de RANGEFLUX y WORLDGRASSAGRIFLUX complementado por 46 sitios desde el conjunto de datos FLUXNET La Thuile divididos mediante el método de respuesta de temperatura (Reichstein, M., E. Falge, D. Baldocchi, D. Papale, R. Valentini, M. Aubinet, P.

Research was supported in part by the Science Applications International Corporation, Subcontract 4400089887 to Gilmanov Research and Consulting, LLP. Measurements at the Alinya site, Spain, Fundación CEAM were partly supported by Generalitat Valenciana, Bancaja, and the Programm CONSOLIDER-INGENIO 2010 (GRACCIE).

This publication was made possible through support provided to the Global Livestock Collaborative Research Support Program by the Office of Agriculture, Bureau for Economic Growth, Agriculture and Trade, United States Agency for International Development under terms of Grant No. PCE-G-00-98-00036-00. The opinions expressed herein are those of the author(s) and do not necessarily reflect the views of the USAID.

Correspondence: Tagir G. Gilmanov, Dept of Biology and Microbiology, South Dakota State University, SAG 305, Box 2207B, Brookings, SD 57006, USA. Email: tagir.gilmanov@sdstate.edu

Manuscript received 6 June 2009; manuscript accepted 13 July 2009.

Berbigier, C. Bernhofer, N. Buchmann, M. Falk, T. Gilmanov, A. Granier, T. Grünwald, K. Havránková, D. Janous, A. Knohl, T. Laurela, A. Lohila, D. Loustau, G. Matteucci, T. Meyers, F. Miglietta, J. M. Ourcival, D. Perrin, J. Pumpanen, S. Rambal, E. Rotenberg, M. Sanz, J. Tenhunen, G. Seufert, F. Vaccari, T. Vesala, and D. Yakir. 2005. On the separation of net ecosystem exchange into assimilation and ecosystem respiration: review and improved algorithm. *Global Change Biology* 11:1424–1439). Los valores máximos del rendimiento cuántico ($\alpha = 75$ mmol · mol^{-1}), capacidad de fotosíntesis (A_{max} =&hairsp3.4 mg CO_2 m^{-2} s^{-1}), fotosíntesis bruta ($P_{g,max} = 116$ g CO_2 m^{-2} d^{-1}), y la eficiencia ecológica de uso de la luz de praderas ($\varepsilon_{ecol} = 59$ mmol · mol^{-1}) manejadas y tierras de cultivo con alto nivel de producción ha superado los de la mayoría de los ecosistemas forestales, esto indica el potencial de los ecosistemas no forestales para la absorción de CO_2 atmosférico. Los valores máximos de producción primaria bruta (8 600 g CO_2 m^{-2} yr^{-1}), la respiración total del ecosistema (7 900 g CO_2 m^{-2} yr^{-1}) y el intercambio de CO_2 neto (2 400 g CO_2 m^{-2} yr^{-1}) se observaron para pastizales manejados intensamente y cultivos de alto rendimiento y son comparables o superiores a los de los ecosistemas forestales, con exclusión de algunos bosques tropicales. En promedio, 80% de los sitios no forestales eran evidentes los sumideros de CO_2 atmosférico, con un promedio neto de absorción de 700 g CO_2 m^{-2} yr^{-1} para pastizales manejados intensivamente y 933 g CO_2 m^{-2} yr^{-1} para tierras de cultivo. Sin embargo, parte de estos aparentes sumideros se acumulan en los cultivos y forrajes, que son reservorios de carbono que son cosechados, transportados y descompuestos fuera del sitio. Por lo tanto, aunque los campos agrícolas pueden ser predominantemente sumideros de CO_2 atmosférico, esto no implica que necesariamente estén aumentando sus reservas de carbono.

Key Words: croplands, ecosystem respiration, grasslands, gross primary production, light-response function method, net CO_2 flux partitioning, net ecosystem CO_2 exchange

INTRODUCTION

Quantifying the contribution of different ecosystems to total regional, continental, and global stocks and exchanges of carbon has been recognized as a fundamental task since the initiation of the carbon cycle science (Rodin and Bazilevich 1968; Whittaker and Likens 1973; Lieth 1975; Olson et al. 1983). Generalizations concerning the role of forest, wetland, and tundra ecosystems in the global carbon budget have been provided recently and have resulted in a general consensus on the contribution of these ecosystem types to the carbon budget (Griffiths and Jarvis 2005; Davidson and Janssens 2006; Birdsey et al. 2007; Bridgham et al. 2007; Tarnocai et al. 2007). Considerably less agreement exists, however, with respect to grassland and cropland ecosystems.

Available estimates of carbon budgets at the country or continental levels typically characterize grasslands as weak sinks, or as approaching a carbon-neutral state, whereas croplands are considered moderate to strong sources of atmospheric carbon (Smith and Falloon 2005; Conant et al. 2007). It should be emphasized, however, that those assessments are not based on direct measurements of carbon exchange, but rather on indirect measures, such as biomass and soil organic matter inventories. Generally, indirect assessments involve combining agricultural fields, where organic matter is produced, with locations (feedlots, harvest processing plants, ethanol facilities, etc.) where harvested biomass is transported and utilized.

Although useful as an initial approximation, indirect measures need to be supplemented with additional data to understand the precise contributions of various land areas to regional atmospheric CO_2 exchange. The objective of our study was to obtain reliable, measurement-based estimates of CO_2 fluxes into and out of the system at the ecosystem scale from CO_2 flux-tower records. Some authors consider maize (*Zea mays* L.) fields that produce grain harvests with little or no soil organic matter loss due to advanced agronomic practices, when considered together with ethanol-producing plants where this corn is processed, as only small net sinks for atmospheric CO_2 (Powlson et al. 2005; Farrell et al. 2006) or even as net carbon sources (Patzek et al. 2005). However, the anthropogenic use of fixed carbon confounds the fact that the site is often a very strong sink for atmospheric CO_2 (e.g., Buyanovsky and Wagner 1998; Bernacchi et al. 2006; Aubinet et al. 2009). Although managed agroecosystems may exhibit sink strength for atmospheric CO_2, anthropogenic harvesting of the fixed carbon products (or erosion) may substantially alter the long-term carbon dynamics at particular sites (similar to timber harvesting in forests). Because decisions concerning the fate of the removed biomass are typically made by humans, opportunities may exist for substantial net sequestration of carbon in grasslands and croplands.

The number and duration of CO_2 flux observations from nonforest flux-tower stations throughout the world have grown exponentially during the last decade. Through the La Thuile synthesis process of the FLUXNET network (Agarwal et al. 2008; Baldocchi 2008b) and other cooperative initiatives, these observations are now available for comparative analysis and generalization. In this publication, we present a synthesis of results from tower CO_2 flux measurements at 118 tower sites representing grassland, cropland, shrubland, savanna, and wetland ecosystems of the world. We first describe the methodology used to derive the terms of the carbon balance used in the global ecosystem comparison, then compare characteristics of the global ecosystem carbon cycle, such as seasonal light responses and CO_2 uptake of nonforest and forest ecosystems. Our objective was to obtain measurement-based estimates of the role of nonforest ecosystems as net sinks or sources for atmospheric CO_2. Such estimates may provide a basis for establishing carbon credit markets and poverty alleviation projects.

METHODS

Data for this study were provided by the WORLDGRASSAGRIFLUX data set (Gilmanov and WORLDGRASSAGRIFLUX Data Set Participants 2007), which currently includes data from 72 nonforest sites (Table 1, method L) for which original 30-min (or 20-min in some sites) net CO_2 flux (F_c) was

Table 1. Nonforest flux-tower sites analyzed in this study.

Site	Latitude	Longitude	Elevation	PCPN	T_{year}	Years	Investigator(s)	Method[1]
Croplands								
Ames, IA, USA, maize	41.720	− 93.410	300	814	8.9	2003	J. Prueger	L
Auradé, France	43.549	1.108	243	690	13.3	2005	E. Ceschia, P. Béziat	T
Batavia-agro, IL, USA	41.859	− 88.223	227	921	10.5	2005–2006	R. Matamala; D. Cook	T
Bondville, IL, USA, maize	40.006	− 88.292	300	990	11.3	1997–2005	S. Hollinger; C. Bernacchi, T. Meyers	L
Bondville, IL, USA, soybeans	40.006	− 88.292	300	990	11.3	1998–2006	S. Hollinger; C. Bernacchi, T. Meyers	L
Bondville-companion, IL, USA	40.006	− 88.292	219	990	11.3	2005–2006	S. Hollinger; C. Bernacchi	T
Borgo Cioffi-crop, Italy	40.524	14.957	20	490	19.0	2004–2006	V. Magliulo	T
Carlow, Ireland	52.859	− 6.918	59	824	9.4	2004–2006	M. Jones; G. Lanigan	L
Doulun, China	42.046	116.280	1 350	399	3.3	2005–2006	Shiping Chen	L
Foulum, maize, Denmark	56.484	9.587	51	712	8.0	2005	J. Olesen; K. Schelde	T
Gebesee, Germany	51.100	10.914	162	492	9.6	2004–2006	C. Rebmann, W. Kutsch	T
Grignon, France	48.844	1.952	125	600	11.1	2005–2006	P. Cellier	T
Haller, PA, USA	48.860	− 77.840	352	974	9.7	2003	R. H. Skinner	L
Klingenberg, Germany	50.893	13.522	480	850	7.0	2004–2006	C. Bernhofer; T. Gruenwald	T
Lamasquère, France, irrigated	43.493	1.237	180	690	13.3	2005	E. Ceschia, P. Béziat	T
Langerak, The Netherlands	52.004	4.806	− 1	805	11.3	2005–2006	E. Moors, J. Elbers, W. Jans	T
Lonzee, Belgium	50.552	4.745	165	800	10.0	2004–2006	C. Moureaux, M. Aubinet	L
Mase, Japan, paddy field	36.054	140.027	13	1 200	13.7	2002–2003	A. Miyata	T
Mead, NE, USA, maize, rainfed	41.180	− 96.440	363	887	9.7	2001–2003	S. Verma, A. Suyker	L
Mead, NE, USA, soybeans, rainfed	41.180	− 96.440	363	887	9.7	2002–2004	S. Verma, A. Suyker	L
Mead, NE, USA, maize rotation, irrigated	41.165	− 96.470	362	887	9.7	2001–2003	S. Verma, A. Suyker	T
Mead, NE, USA, maize, irrigated	41.165	− 96.477	361	728	10.1	2001–2004	S. Verma, A. Suyker	T
Mead, NE, USA, soybeans, irrigated	41.165	− 96.470	362	728	10.1	2002–2004	S. Verma, A. Suyker	T
Molenweg, The Netherlands	51.650	4.639	1	800	9.8	2005	E. Moors, J. Elbers	T
Oensingen, Switzerland	47.286	7.734	452	1 100	9.0	2005	N. Buchmann; W. Eugster	T
Ponca City, OK, USA, winter wheat	36.767	− 97.133	310	866	14.8	1997	S. Verma	L
Risbyholm, Denmark	51.530	12.097	10	575	9.0	2004–2005	H. Soegaard	T
Rosemount, MN, USA	44.714	− 93.090	260	799	6.8	2004–2005	T. Griffis, J. Baker	L
Extensively managed grasslands								
Alinya, Spain	42.152	1.449	1 770	669	13.0	2003–2005	M. J. Sanz, C. Gimeno	L
Amplero, Italy	41.867	13.633	884	1 365	10.0	2003–2005	M. Balzarolo	L
Atquasuk, AK, USA[2]	70.470	− 157.409	N/A	127	NA?	1999–2006	W. Oechel	T
Audubon Ranch, AZ, USA	31.591	− 110.510	985	382	16.0	2002–2006	T. Meyers	L
Barrow, AK, USA[2]	71.323	− 156.626	1	124	− 12.5	1998–2002	W. Oechel	T
Batavia Prairie, IL, USA	41.841	− 88.241	226	921	10.5	2005–2006	R. Matamala	L
Bily Kriz, Czech Republic	49.495	18.545	855	1 200	5.5	2004–2006	M. Marek, R. Czerny	T
Brookings, SD, USA	44.311	− 96.798	495	550	5.8	2004–2006	T. Meyers, T. Gilmanov, M. Heuer	L
Bugacpuszta, Hungary	46.691	19.601	113	562	10.4	2003–2006	Z. Nagy, K. Pinter	L
Canaan Valley, WV, USA	39.063	− 79.421	988	900	8.2	2004	T. Meyers	L
Cheyenne, WY, USA	41.183	− 104.900	1 910	397	7.2	1997–1998	J. Morgan	L
Cottonwood, SD, USA	43.950	− 101.847	735	447	7.7	2004–2006	T. Meyers, A. Detwiler, K. Brehe	L
Central Plains Experimental Range, CO, USA	40.683	− 104.750	1 660	332	9.2	2001–2004	J. Morgan	L
Doulun, China	42.047	116.284	1 350	399	3.3	2006	Shiping Chen	L
Duke grassland, NC, USA	35.971	− 79.090	163	1 145	15.5	2001–2005	G. Katul, P. C. Stoy, K. A. Novick	L
Fort Peck, MT, USA	48.308	− 105.101	634	310	7.7	2000–2006	T. Meyers	L
Fort Reno, OK, USA	35.557	− 98.017	421	870	14.9	2005	M. Torn, D. Billesbach	L
Freeman Ranch, TX, USA	29.930	− 98.010	244	959	19.4	2004	J. Heilman	L
Goodwin Creek, MS, USA	34.250	− 89.970	70	1 455	15.7	2002–2006	T. Meyers	L

Table 1. Continued.

Site	Latitude	Longitude	Elevation	PCPN	T_{year}	Years	Investigator(s)	Method[1]
Grillenburg, Germany	50.951	13.514	380	853	7.2	2004–2006	C. Bernhofer, T. Gruenwald	L
Gudmundsen Ranch, NE, USA	42.069	− 101.407	1 081	560	7.9	2006	D. Billesbach	L
Haibei, China	37.617	101.317	3 250	561	− 1.7	2002–2003	T. Kato	T
Ivotuk, AK, USA	68.486	− 155.750	550	250	− 9.0	2004–2006	W. Oechel	T
Jornada, NM, USA	32.600	− 106.750	1 320	272	N/A	2000–2001	W. Dugas, P. Mielnick	L
Karnap, Uzbekistan	40.000	65.500	310	237	14.6	2001	M. Nasyrov, N. Saliendra	L
Kendall, AZ, USA	31.737	− 109.942	1 531	356	17.0	1999–2006	W. Emmerich	L
Khakasia, Russia	54.773	90.002	430	388	2.2	2002–2004	L. Belelli	L
Khakasia 3, Russia	54.705	89.078	401	384	2.3	2004	L. Belelli	T
Kherlenbayan-Ulaan, Mongolia	47.214	108.737	1 235	196	1.2	2003	Shenggong Li	L
Laqueuille, France	45.643	2.736	1 040	1 013	8.6	2002–2006	J.-F. Soussana, V. Allard	L
Lethbridge, Canada	49.709	− 112.940	960	378	6.4	1998–2002	L. Flanagan	L
Little Washita, OK, USA	34.967	− 97.983	335	750	16.3	1997–1998	T. Meyers	L
Malga Arpaco, Italy	46.117	11.703	1 699	1 200	6.3	2003–2004	A. Raschi	L
Mandan, ND, USA	46.767	− 100.917	518	404	5.0	1999–2001	A. Frank	L
Matra, Hungary	47.842	19.726	350	622	10.2	2004–2005	Z. Tuba, Z. Nagy, J. Balogh	T
Miles City, MT, USA	46.300	− 105.967	719	343	7.9	2000–2001	M. Haferkamp	L
Monte Bondone, Italy	46.016	11.047	1 550	1 189	5.5	2003–2006	D. Gianelle	T
Neal Smith, IA, USA	41.558	− 93.296	280	826	9.1	2005	J. Prueger	L
Oensingen, Switzerland	47.286	7.732	452	1 100	9.0	2002–2003	C. Ammann, J. Fuhrer	L
Rannels Ranch, KS, USA	39.139	− 96.523	324	840	12.9	1998–1999	C. Owensby	L
Rigi-Seebodenalp, Switzerland	47.058	8.457	1 025	1 327	7.3	2003	W. Eugster, N. Rogiers	L
Rondonia, Brazil	− 10.762	− 62.357	306	1 664	23.9	1999	M. Waterloo, A. Manzi	L
Santarem, Brazil	− 3.012	− 54.537	N/A	N/A	N/A	2001–2002	D. Fitzjarrald	L
Shidler, OK, USA	36.933	− 96.683	356	942	14.8	1997–1999	S. Verma, A. Suyker	L
Shortandy, Kazakhstan	51.667	71.000	367	323	1.6	1998–2001	K. Akshalov, N. Saliendra, D. A. Johnson	L
Temple, TX, USA	31.100	− 97.333	219	878	19.6	1998–1999	W. Dugas, P. Mielnick	L
Tojal, Portugal	38.477	− 8.025	190	669	15.5	2004–2006	C. Pio, L. Aires	L
Viara Ranch, CA, USA	38.407	− 120.951	129	500	15.9	2001–2006	D. Baldocchi	L
Walnut River, KS, USA	37.521	− 96.855	408	1 030	13.1	2002–2004	R. Coulter, D. Cook	L
Woodward, OK, USA	36.600	− 99.583	630	586	14.3	1997–2002	P. Sims, J. Bradford	L
Xilinhot grazed, China	43.554	116.671	1 250	360	2.0	2006	Shiping Chen	L
Xilinhot, fenced, China	43.546	116.678	1 250	360	2.0	2006	Shiping Chen	T
Xilinhot, typical fenced, China	44.134	116.329	1 030	290	2.0	2004–2006	Guangsheng Zhou	T
Intensively managed grasslands								
Cabauw extension, the Netherlands	51.954	4.903	− 1	786	9.8	2005	E. Moors, J. Elbers	T
Cabauw, the Netherlands	51.967	4.917	− 1	800	10.0	2003	A. Hensen	T
Cabauw, the Netherlands	51.971	4.927	− 1	786	9.8	2004–2006	E. Moors, J. Elbers, F. Bosveld	T
Carlow, grassland, Ireland	52.850	− 6.900	50	804	10.1	2003	M. Jones, G. Lanigan	L
Dripsey, grass, Ireland	51.919	− 8.751	187	1 450	9.5	2002–2005	G. Kiely, P. Leahy	T
Easter Bush, United Kingdom	55.867	− 3.200	190	890	8.0	2003–2004	M. Sutton	L
Haarweg, the Netherlands	51.970	5.630	7	760	9.5	2002	A. Jacobs	T
Haastrecht, the Netherlands	52.004	4.806	− 2	786	9.8	2003	E. Moors	T
Haller, PA, USA	40.862	− 77.840	352	974	9.7	2003–2005	R. H. Skinner	L
Hegyhátsál, Hungary	46.950	16.650	248	759	8.9	1999	Z. Barcza, L. Haszpra	T
Horstermeer, the Netherlands	52.029	5.068	− 2	797	9.8	2004–2006	A. J. Dolman	T
Jokioinen, Finland	60.899	23.514	104	581	3.9	2002	A. Lohila, T. Laurila	L
Lacombe, Canada	52.436	− 113.808	871	446	2.1	2003	V. S. Baron	L
Laqueuille, France	45.643	2.736	1 040	1 013	8.6	2002–2006	J.-F. Soussana, V. Allard	L
Lelystad, the Netherlands	52.500	5.500	0	780	10.0	2004	A. Hensen	L
Lille Valby, Denmark	55.700	12.117	15	1 119	8.5	2004–2006	E. Dellwik	L
Neustift, Austria	47.117	11.317	970	850	6.3	2001–2006	G. Wohlfahrt	L
Oensingen, Switzerland	47.283	7.733	485	1 100	9.0	2002–2006	C. Ammann; J. Fuhrer	L

Table 1. Continued.

Site	Latitude	Longitude	Elevation	PCPN	T_{year}	Years	Investigator(s)	Method[1]
Shrublands and savanna								
Burns, OR, USA	43.483	− 119.717	1 380	283	7.6	1995–2001	T. Svejcar	L
Dubois, ID, USA	44.267	− 112.133	1 700	302	6.2	1996–2001	D. A. Johnson, N. Z. Saliendra	L
Howard Springs, Australia	− 12.329	131.000	38	1 824	25.9	2002–2005	J. Beringer	L
Karrykul, Turkmenistan	38.600	58.400	90	148	15.6	1998–2000	M. Durikov, N. Saliendra, D. A. Johnson	L
Kubuqi, China	40.381	108.549	1 160	180	7.5	2006	Shiping Chen	L
Santa Rita, AZ, USA	31.821	− 110.866	1 120	330	17.6	2004–2006	R. Scott	T
Sao Paulo, Brazil	− 21.619	− 47.650	N/A	953	N/A	2001–2002	H. da Rocha	T
Skukuza, South Africa	− 24.983	31.600	263	561	21.6	2001–2003	N. Hanan	L
Sky Oaks, CA, USA, old stand	33.374	− 116.623	1 394	491	12.2	1997–2006	W. Oechel	L
Sky Oaks, CA, USA, young stand	33.377	− 116.623	1 429	491	12.2	1997–2001	W. Oechel	T
Tonzi Ranch, CA, USA	38.432	− 120.966	177	559	15.4	2002–2006	D. Baldocchi	T
Wetlands								
Cherskii, Russia	68.615	161.339	4	200	− 12.5	2003–2004	C. Corradi	T
CzechWet, Czech Republic	49.025	14.772	420	740	7.2	2006	M. Marek; D. Janous	T
Dongtan marsh 1, China	31.517	121.961	4	2 192	15.7	2005	Bin Zhao; Haiqiang Guo	T
Dongtan marsh 2, China	31.585	121.903	4	2 074	15.7	2005	Bin Zhao; Guo Haiqiang	T
Dongtan marsh 3, China	31.517	121.972	4	2 190	15.5	2005	Bin Zhao; Haiquang Guo	T
Kaamanen wetland, Finland	69.141	27.295	155	395	− 1.3	2000–2006	T. Laurila; M. Aurela	T
PolWet, Poland	52.762	16.309	54	550	8.1	2004	M. Urbaniak, J. Olejnik	T
Siikaneva, Finland	61.833	24.193	N/A	713	3.0	2004–2006	M. Aurela	T
Tadham Moore, United Kingdom	51.207	− 2.829	3	750	11.1	2001	R. Harding, C. Lloyd	T

[1]Method on net flux partitioning into photosynthesis and respiration: L indicates light-response function analysis; T, nighttime temperature dependence.
[2]Inherently wet Atqasuk and Barrow sites representing zonal tundra communities could not be pooled together with true intrazonal wetlands used in this study and were conditionally classified as "extensive grasslands." Tundra would be separated into a distinct category if sufficient data were available.

partitioned into gross primary productivity (P_g) and ecosystem respiration (R_e) components with the use of light-response function methods (Gilmanov et al. 2003a, 2003b, 2004, 2005, 2006, 2007). These data were combined with an additional 46 nonforest sites (Table 1, method T) from the FLUXNET La Thuile data set (Agarwal et al. 2008) that were partitioned into P_g and R_e components with the use of the temperature-response methods (Reichstein et al. 2005). In most cases, we used daily P_g and R_e estimates directly from the La Thuile data set, though sometimes it was necessary to correct spurious values of daily gross primary production that were occasionally generated by the nighttime temperature-response method owing to the substantial scatter that may exist in instantaneous CO_2 flux measurements (cf. Stoy et al. 2006).

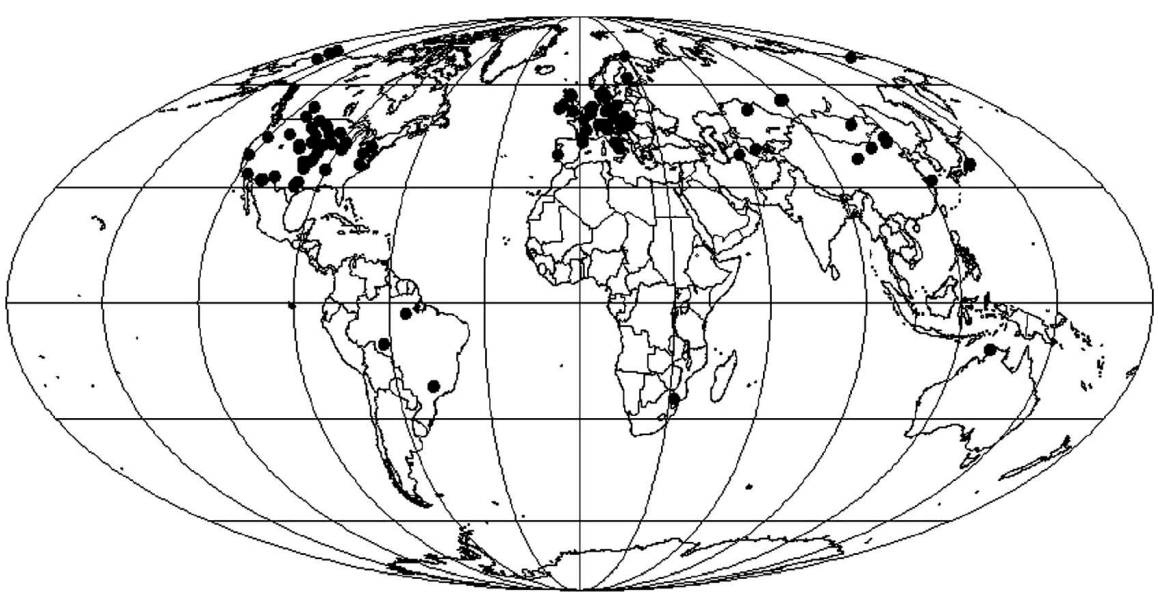

Figure 1. Geographical distribution of the 118 nonforest flux-tower sites considered in this study.

In total, tower sites included in our analysis represented 316 site-years of measurements during the 1997–2006 period (Table 1). They are grouped into the following categories: extensively managed grasslands (ungrazed or lightly grazed, uncut or cut occasionally), intensively managed grasslands (regularly cut, grazed, fertilized, irrigated, etc.), croplands, shrublands/savannas, and wetlands. The geographic distribution of sites is illustrated in Figure 1.

Net Tower Flux F_c Partitioning into Photosynthesis P_g and Respiration R_e

Analysis of flux-tower measurements requires processing algorithms (Lee et al. 2004; Burba and Anderson 2007; Baldocchi 2008a) that describe the net result of interacting ecosystem components that absorb CO_2, mostly photosynthetic assimilation by autotrophic organisms and those that release CO_2 (metabolic CO_2 production, R_e, is the major component of CO_2 efflux in most ecosystems where geologic production of CO_2 does not predominate). Because photosynthesis and respiration respond rather differently to major environmental drivers (e.g., Thornley and Johnson 2000), partitioning of tower-based F_c data into photosynthetic assimilation and ecosystem respiration components is recognized as a necessary step in the postprocessing of net flux data for use in predictive modeling of ecosystem carbon cycling (Gilmanov et al. 2003b, 2004, 2005; Reichstein et al. 2005; Wohlfahrt et al. 2005; Gilmanov et al. 2006; Stoy et al. 2006; Gilmanov et al. 2007).

With the use of the ecophysiological sign convention (positive flux from atmosphere to ecosystem), and excluding plants with CAM-type metabolism, P_g used in this study was obtained as a sum of daytime F_c and daytime ecosystem respiration (R_d), minus the rate of change of CO_2 storage in the atmospheric layer between the soil surface and the CO_2 sensor at the tower (Gilmanov and WORLDGRASSAGRIFLUX Data Set Participants 2007). When estimates of the storage term were not available (e.g., for communities with low canopy height and sufficient turbulent transport) the gross productivity was approximated as

$$P_g(t) = \begin{cases} F_c(t) + R_d(t), & Q(t) > 0 \\ 0, & Q(t) = 0 \end{cases} \quad [1]$$

where $Q(t)$ is the intensity of photosynthetically active radiation (Gilmanov et al. 2004).

Because direct measurements of the R_d are quite difficult to make, two main approaches of its indirect estimation (leading to the two major methods of net flux partitioning into photosynthesis and respiration components) were used. The first approach establishes the relationship of nighttime respiration (R_n),

$$R_n(t) = \begin{cases} F_c(t), & Q(t) = 0 \\ 0, & Q(t) > 0 \end{cases} \quad [2]$$

to environmental drivers affecting it (e.g., soil temperature [T_s]) and uses these relationships to estimate R_d. This approach has been widely used for forest-type ecosystems (Goulden et al. 1996) and was used in this study for the first round of network-level aggregation of the raw 30-min data into daily gross primary productivity and ecosystem respiration values (http://www.fluxdata.org/DataInfo/).

The second approach involves obtaining estimates of R_d through identification of the respiration term in the ecosystem-scale light-response functions describing relationships of the daytime F_c to photon flux density, Q, leaf area index (L), T_s, water content of the soil (W_s), air relative humidity (RH), and other factors. In general, light-response functions include rather complicated analytical or algorithmic expressions (e.g., those suggested by Thornley and Johnson 2000), taking into account most of the major ecophysiological parameters of photosynthesis (quantum yield [α], maximum photosynthesis [A_{max}], convexity of the light response [θ], and L). When fully expanded, these expressions can require several lines of printed text. At the other end of the complexity spectrum lie simple $F_c(Q)$ relationships such as the ramp function by Blackman (1905), Mitscherlich's saturated exponent (1909), and the rectangular hyperbola by Tamiya (1951), the latter being a nearly standard approach to light-response fitting at the early stages of flux-tower data analysis (Ruimy et al. 1995). These simple models are convenient and, in some cases, fit observed data well; however, they share the major drawback of lacking the ability to describe light-response patterns of varying convexity (curvature).

Under the widely accepted ecophysiological framework, the convexity of the light response is represented by the fraction of diffusion resistance to the total (diffusion + carboxylation) resistance to carbon transport: $\theta = \rho_d/(\rho_d + \rho_x)$; Thornley and Johnson 2000). If the differences in leaf morphology and biochemistry in different plant groups are taken into account (e.g., C_3 vs. C_4 photosynthesis types), the ability to describe light-response curves of different convexity seems to be a necessary requirement for an adequate light-response function model. Our experience with quantification of the tower-based light-response data from a wide range of nonforest ecosystems led us to use the nonrectangular hyperbolic model (Rabinowich 1951; Thornley and Johnson 2000):

$$F_c(Q;\alpha,A_{max},\theta,r_d) = \frac{1}{2\theta}\left(\alpha Q + A_{max} - \sqrt{(\alpha Q + A_{max})^2 - 4\alpha A_{max}\theta Q}\right) - r_d, \quad [3]$$

where Q denotes photon flux density, α is the quantum yield, A_{max} is maximum gross photosynthesis, θ is the convexity parameter of the light-response curve, and r_d is daytime ecosystem respiration rate for days when solar radiation is the major driver of daytime CO_2 exchange. This model provides a powerful and flexible tool to describe light response at the various nonforest tower sites (Gilmanov et al. 2003a, 2003b, 2004, 2005, 2006, 2007).

Under semiarid and arid conditions, when significant warming of the soil in the afternoon period is observed, the pattern of data points on the light-response plane {Q, F_c} is often characterized by a hysteresis-like loop with the morning branch of the light-response curve lying above the afternoon branch. In such cases, these light-response patterns were effectively described by the modified nonrectangular hyperbolic model (Gilmanov et al. 2003a):

$$F_c(Q,T_s;\alpha,A_{max},\theta,r_d) = \frac{1}{2\theta}\left(\alpha Q + A_{max} - \sqrt{(\alpha Q + A_{max})^2 - 4\alpha A_{max}\theta Q}\right) - r_0 e^{k_T T_s}, \quad [4]$$

where the daytime respiration term r_d of Equation [3] is modified to $r_0 e^{k_T T_s}$ to represent an exponential increase of respiration with soil temperature, T_s and k_T and r_0 are empirical parameters estimated by fitting Equation 4 to the daytime data $\{Q(t_i), T_s(t_i), F_c(t_i)\}$, and t_i is time between the sunrise and sunset, $t_r \leq t_i \leq t_s$. For days described by Equation 4, average daytime respiration rate, r_d, was calculated as

$$r_d = \frac{r_0}{t_s - t_r}\int_{t_r}^{t_s} e^{k_T T_s(t)}\, dt. \quad [5]$$

In cases where vapor pressure deficit (VPD) effect limits CO_2 uptake, this approach would tend to overestimate r_d, and consequently P_g, when a decline of P_g may be just as likely. Numerical fitting of parameters α, A_{max}, θ, r_d, or r_0 and k_T of Equations 3 or 4 was achieved using procedures from the Global Optimization Package (Loehle Enterprises 2007) available under the Mathematica software system (Wolfram Research 2009). It should be emphasized that to avoid serious errors in estimating light-response parameters resulting from fitting equations to data pooled across over several days (as sometimes can be seen in publications on the subject, e.g., Ruimy et al. 1995; Zhang et al. 2006; Zhao et al. 2006), only single-day data sets $\{Q(t_i), T_s(t_i), F_c(t_i)\}$ were used in this study to identify the light curves and the light–temperature response surfaces of CO_2 exchange.

It should also be noted that parameters obtained by fitting Equations 3 or 4 to flux-tower data sets are ecosystem-scale parameters referring to a ground unit (e.g., per 1-m^2 ground surface) and should be distinguished from leaf-level light-response parameters used in physiological studies, which correspond to units of leaf area (e.g., $A_{L,max}$, α_L, etc.). Only under special conditions (monoculture with convexity $\theta = 0$), is photosynthetic capacity per unit ground area (A_{max}) equal to the product of photosynthetic capacity per unit leaf area ($A_{L,max}$) and the leaf area index (L): $A_{max} = A_{L,max} \times L$ (cf. Thornley and Johnson 2000).

For measurement days that allow identification of parameters of models [3] or [4], total R_d was calculated as the product of average r_d and the length of the daylight period:

$$R_d = r_d(t_s - t_r). \quad [6]$$

For days with daytime data inappropriate for light-response analysis, parameters k_T and r_0 were estimated by fitting an exponential equation $F_c = r_0 e^{k_T T_s}$ to the nighttime data, $\{T_s(t_i), F_c(t_i)\}_{Q(t_i)=0}$.

Eventually, total daily gross primary production (P_g) was obtained as the sum of daytime respiration total (R_d) and the daytime net flux integral, $P_d = \int_{t_r}^{t_s} F_c(t)\, dt$ $P_d = \int_{t_r}^{t_s} F_c(t)\, dt$:

$$P_g = P_d + R_d. \quad [7]$$

Gap-filling of P_g and R_e values for days with missing measurements was achieved with the use of various methods characterized in the recent review by Moffat et al. (2007), with particular emphasis on 1) extrapolation of parameters of light- and temperature-response functions to days with missing flux measurements, calculations of fluxes at the 30-min time scale, and estimation of daily P_g and R_e values as integrals of corresponding 30-min estimates; and 2) nonlinear regressions of daily P_g and R_e values from daily aggregated values of predictors such as photosynthetically active radiation, air and soil temperature, soil water content, etc.

Seasonal Patterns of Parameter Dynamics

Numerical estimation of the major light-response parameters on a daily basis, i.e., obtaining the values α, A_{max}, θ, r_d for as many days t as allowed by the quality and quantity of the data, permits evaluation of time-functions $\alpha(t)$, $A_{max}(t)$, $\alpha(t)$, $r_d(t)$ characterizing seasonal patterns of the dynamics of these parameters. These patterns are revealed most clearly through smoothing of the empirical time series of the parameter estimates. In this study, we used one of the simplest and easily interpretable methods—calculation of the mean parameter value and its standard error, e.g., $\{\overline{\alpha}_j, s_{\overline{\alpha}_j}\}$, $\{\overline{A}_{max}, j, s_{\overline{A}_{max},j}\}$, etc. for every calendar week j of the year of observations (j 1,…, 52}. Using weekly average values instead of individual daily estimates is effective for comparison among ecosystems and years, particularly for such parameters as quantum yield (α), which exhibits large day-to-day variability.

Seasonal Dynamics and Annual Budgets of Annual Gross Primary Production (GPP), Annual Total Ecosystem Respiration (RE), and Net Ecosystem CO_2 Exchange (NEE)

Estimated values of $P_g(t)$ and $R_e(t)$ for the year-round or observation period were integrated across 365 days (or across measurement season when no year-round data were available) to obtain annual (seasonal) totals of GPP and RE. Integrated NEE total to day t, IntNEE(t), was calculated by integrating daily values of $F_c(t) = P_g(t) - R_e(t)$. NEE was calculated as the difference between GPP and RE.

Ecosystem-Scale Light-Use Efficiency

Comparative physiological studies at the leaf, individual, or population level commonly calculate the light-use efficiency of gross photosynthesis (P_g) with respect to absorbed photosynthetically active radiation, Q_a, resulting in a gross physiological light-use efficiency coefficient (Larcher 1995):

$$\varepsilon_{phys} = \frac{P_g}{Q_a}, \quad [8]$$

where both the photosynthesis P_g and absorbed radiation Q_a are expressed in molar units (e.g., it is convenient to measure ε in mmol CO_2 per mol quanta). However, in comparative ecological studies it is preferable to use the coefficient of gross ecological light-use efficiency (cf. Odum 1959 [p. 54]; Cooper 1970; Austin et al. 1978; Colinvaux 1993):

$$\varepsilon_{ecol} = \frac{P_g}{Q}, \quad [9]$$

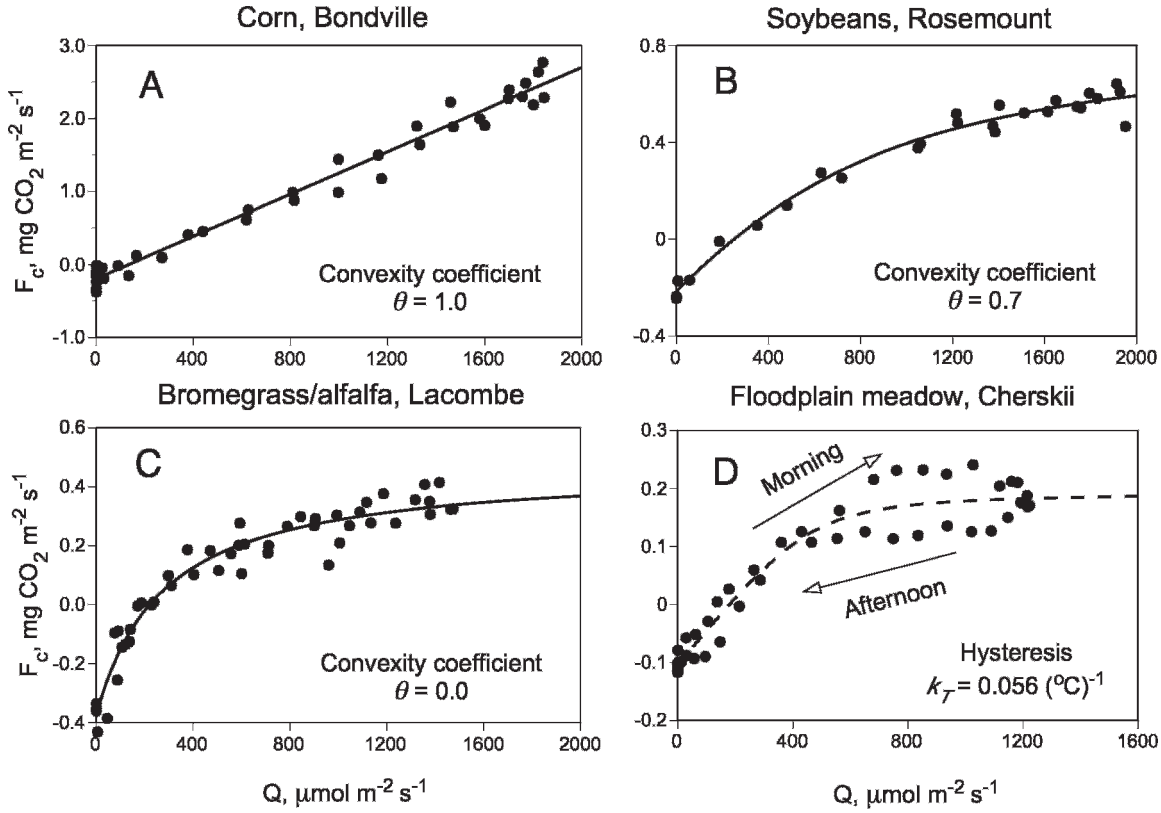

Figure 2. Major types of ecosystem light-response functions: **A**, linear, convexity $\theta = 1$ (maize crop, Bondville, IL, USA, 1999, day 188); **B**, nonrectangular hyperbolic, convexity $0 < \theta < 1$ (soybeans, Rosemount, MN, USA, 2004, day 207); **C**, rectangular hyperbolic, $\theta = 0$ (meadow bromegrass/alfalfa, Lacombe, Alberta, Canada, 2003, day 151); **D**, hysteresis (floodplain meadow, Cherskii, East Siberia, Russia, 2005, day 1 900, $k_T = 0.056\ ^\circ C^{-1}$).

calculated per unit of *total incoming* photosynthetically active radiation, Q. Although the physiological light-use efficiency coefficient, ε_{phys}, characterizes physiological and biochemical parameters (and is often used in studies performed at the unit leaf area or unit of photosynthetically active biomass basis), the ecological light-use efficiency, ε_{ecol}, as a rule, is calculated per unit ground surface (m^{-2}, ha^{-1}, etc.), and thus also takes into account such ecosystem-level properties as population density, aboveground biomass, and leaf area.

RESULTS AND DISCUSSION

Light-Response Functions and Parameters

Within the broad range of climatic conditions and ecosystem types represented in the data set, we observed a variety of patterns of light response. For comparative purposes, it is convenient to distinguish four major categories differentiated in terms of convexity and presence of the hysteresis-like loop on the light-response scatter diagram $\{Q,F_c\}$ (Fig. 2). In the latter case, plotting the 3-D scatter diagram of the diurnal dynamics of the measurement data and of the response surface $F_c(Q,T_s)$ (Equation 4) fitted to them provides a partial explanation of the loop on the 2-D $\{Q,F_c\}$ plot caused by the increase of ecosystem respiration with the increase of temperature in the afternoon hours (Fig. 3). For the cases shown in Figures 2 and 3, numerical estimates and statistical characteristics of parameters in Equations 3 and 4 are presented in Tables 2 and 3.

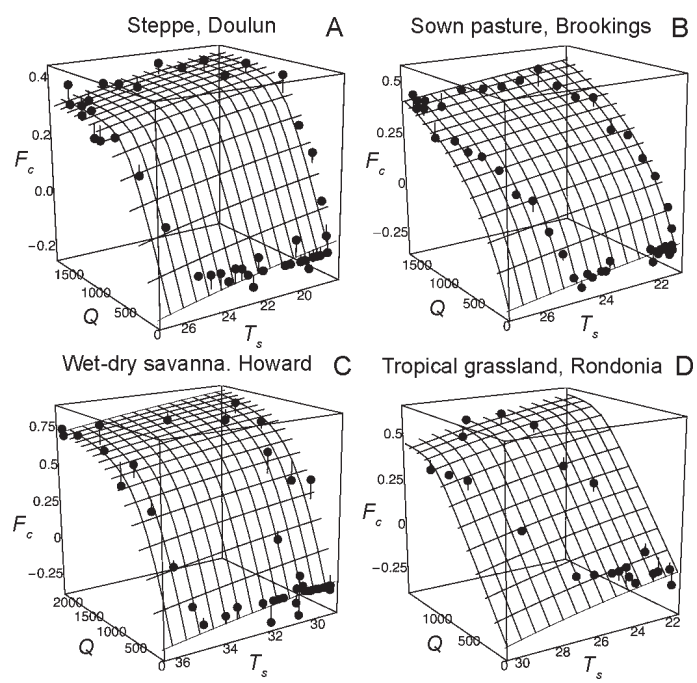

Figure 3. Light-temperature response surfaces fitted by modified nonrectangular Equation 4 for representative days for **A**, Doulun steppe, China, 2006, day 218; **B**, Brookings sown pasture, SD, USA, 2005, day 190; **C**, Howard wet-dry savanna, Australia, 2002, day 34; and **D**, Rondonia tropical grassland, Brazil, 1999, day 270.

Table 2. Parameters α, A_{max}, r_d, and θ from the nonrectangular hyperbolic light-response function $F_c(Q) = (1/\theta)\left(\alpha Q + A_{max} - \sqrt{(\alpha Q + A_{max})^2 - 4\alpha A_{max}\theta Q}\right) - r_d$ for representative days at the Bondville, Rosemount, Lacombe, and Brookings flux-tower stations.

Statistical characteristics	Parameters			
	Slope, α mg $CO_2 \cdot \mu mol^{-1}$	Plateau, A_{max} mg $CO_2 \cdot m^{-2} \cdot s^{-1}$	Respiration, r_d mg $CO_2 \cdot m^{-2} \cdot s^{-1}$	Convexity, θ dimensionless
Maize crop, Bondville, IL, USA, 1999, day 188; $R^2 = 0.98$; SE = 0.158 mg $CO_2 \cdot m^{-2} \cdot s^{-1}$				
Estimate	0.0014	3.2	0.1936	1.0
Standard error	0.0001	–	0.0423	0.0012
Student's *t*	19.92	–	4.58	84.20
P level	0.0000	–	0.0000	0.0000
Soybeans, Rosemount, MN, USA, 2004, day 207; $R^2 = 0.98$; SE = 0.045 mg $CO_2 \cdot m^{-2} \cdot s^{-1}$				
Estimate	0.0009	0.9930	0.2002	0.6947
Standard Error	0.0002	0.1899	0.0221	0.3329
Student's *t*	4.77	5.23	9.07	2.09
P level	0.0000	0.0000	0.0000	0.0243
Sown pasture, Lacombe, Alberta, Canada, 2003, day 151; $R^2 = 0.94$; SE = 0.061 mg $CO_2 \cdot m^{-2} \cdot s^{-1}$				
Estimate	0.0026	0.8321	0.3413	0.0
Standard error	0.0009	0.0969	0.0273	–
Student's *t*	2.98	8.58	12.50	–
P level	0.0023	0.0000	0.0000	–
Floodplain meadow, Cherskii, East Siberia, Russia, 2003, day 214; $R^2 = 0.93$; SE = 0.033 mg $CO_2 \cdot m^{-2} \cdot s^{-1}$				
Estimate	0.0006	0.2987	0.1038	0.9333
Standard error	0.0001	0.0252	0.090	0.090
Student's *t*	5.31	11.85	11.58	10.38
P level	0.0000	0.0000	0.0000	0.0000

Table 3. Parameters α, A_{max}, r_0, k_T, and θ from the modified nonrectangular hyperbolic light-temperature response function $F_c(Q, T_s) = (1/2\theta)\left(\alpha Q A_{max}\sqrt{(\alpha Q A_{max})^2 4\alpha A_{max}\theta Q}\right) - r_0 e^{k_T T_s}$, for representative days at Doulun, Brookings, Howard, and Rondonia sites.

Statistical characteristics	Parameters				
	Slope, α mg $CO_2 \cdot \mu mol^{-1}$	Plateau, A_{max} mg $CO_2 \cdot m^{-2} \cdot s^{-1}$	Respiration, r_0 mg $CO_2 \cdot m^{-2} \cdot s^{-1}$	Temperature coefficient, k_T, $(^\circ C)^{-1}$	Convexity, θ dimensionless
Steppe, Doulun, China, 2006, day 218; $R^2 = 0.98$; SE = 0.037 mg $CO_2 \cdot m^{-2} \cdot s^{-1}$					
Estimate	0.0009	0.5542	0.0377	0.0671	0.9644
Standard error	0.00001	0.0241	0.0102	0.0116	0.0408
Student's *t*	9.08	22.98	3.68	5.78	23.64
P level	0.0000	0.0000	0.0003	0.0000	0.0000
Sown pasture, Brookings, SD, USA, 2005, day 190; $R^2 = 0.99$; SE = 0.032 mg $CO_2 \cdot m^{-2} \cdot s^{-1}$					
Estimate	0.0014	1.0867	0.0631	0.0614	0.0000
Standard error	0.0001	0.0498	0.0141	0.0094	0.0000
Student's *t*	13.87	21.81	4.48	6.53	–
P level	0.0000	0.0000	0.0000	0.0000	–
Wet-dry savanna, Howard, Australia, 2002, day 34; $R^2 = 0.97$; SE = 0.074 mg $CO_2 \cdot m^{-2} \cdot s^{-1}$					
Estimate	0.0017	1.147	0.0278	0.0690	0.8376
Standard error	0.0003	0.1019	0.0167	0.0186	0.1529
Student's *t*	5.83	11.25	1.67	3.71	5.48
P level	0.0000	0.0000	0.0522	0.0004	0.0000
Tropical grassland, Rondonia, Brazil, 1999, day 270; $R^2 = 0.97$; SE = 0.052 mg $CO_2 \cdot m^{-2} \cdot s^{-1}$					
Estimate	0.0008	0.8048	0.0339	0.0760	0.9902
Standard error	0.0001	0.0721	0.0183	0.0217	0.0230
Student's *t*	9.38	11.16	1.85	3.50	43.04
P level	0.0000	0.0000	0.0408	0.0014	0.0000

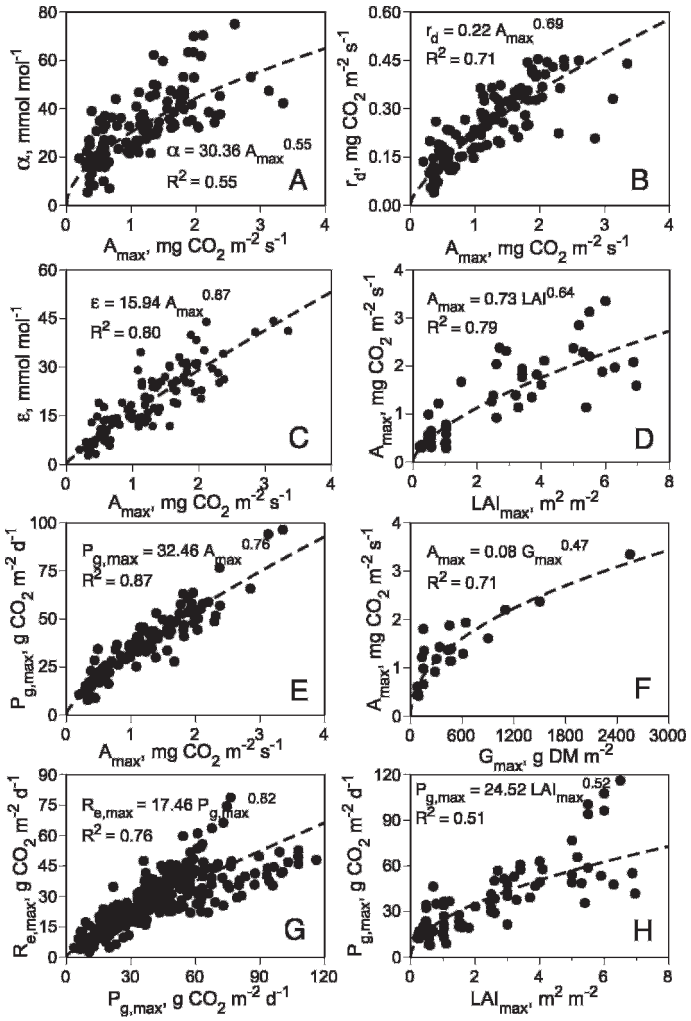

Figure 4. Scatter diagrams of maximum weekly values of light-response (α, A_{max}, $P_{g,max}$, L_{max}), metabolic (r_d, $R_{e,max}$), and efficiency (ε, G_{max}) parameters for the pooled data set including grasslands (extensively and intensively managed), shrublands and savannas, wetlands, and croplands: **A**, α vs. A_{max}; **B**, r_d vs. A_{max}; **C**, ε vs. A_{max}; **D**, A_{max} vs. L_{max}; **E**, $P_{g,max}$ vs. A_{max}; **F**, A_{max} vs. G_{max}; **G**, $R_{e,max}$ vs. $P_{g,max}$; and **H**, $P_{g,max}$ vs. L_{max}. Dashed lines describe linear or power law equations characterizing patterns of covariation between parameters. See list of symbols for definitions.

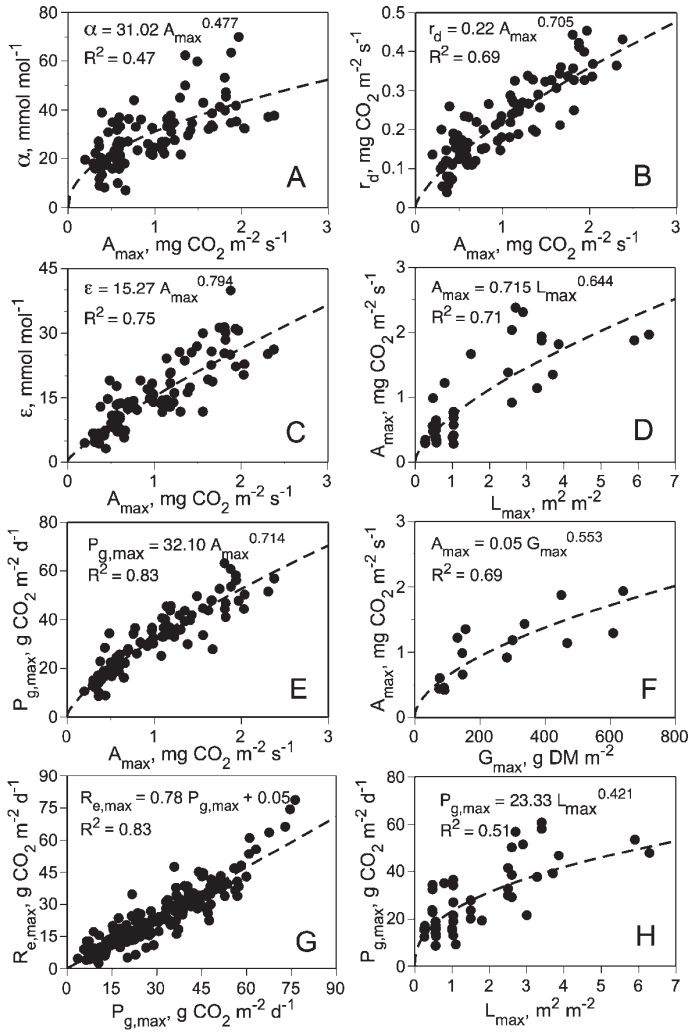

Figure 5. Scatter diagrams of maximum weekly values of light-response (α, A_{max}, $P_{g,max}$, L_{max}), metabolic (r_d, $R_{e,max}$), and efficiency (ε, G_{max}) parameters for the extensively managed grasslands data subset: **A**, α vs. A_{max}; **B**, r_d vs. A_{max}; **C**, ε vs. A_{max}; **D**, A_{max} vs. L_{max}; **E**, $P_{g,max}$ vs. A_{max}; **F**, A_{max} vs. G_{max}; **G**, $R_{e,max}$ vs. $P_{g,max}$; and **H**, $P_{g,max}$ vs. L_{max}. Dashed lines describe linear or power law equations characterizing patterns of co-variation between parameters. See list of symbols for definitions.

The nonrectangular hyperbolic Equation 3 and its modification (Eq. 4) that takes into account the temperature dependence of daytime respiration were good numerical tools for fitting light responses of nonforest ecosystems for days when photosynthetically active radiation was the dominant factor governing ecosystem CO_2 exchange. It is important to emphasize that the nonrectangular hyperbola provided a close fit to light-response data and provided consistent estimates of the light-response parameters for days when the $\{Q,F_c\}$ plots showed no saturation with respect to Q and were characterized by convexity parameter θ close to 1 (cf. Fig. 2A). The rectangular hyperbola, Mitscherlich's equation, and other approximations that lacked the convexity parameter fitted to data with such a pattern yielded highly biased estimates of the initial slope, plateau, and the intercept parameters.

Estimates of apparent quantum efficiency, α, in nonforest ecosystems cover a wide range of values (Fig. 4A) from 5 $mmol \cdot mol^{-1}$ in the desert shrublands of Central Asia (Karrykul) to 75 $mmol \cdot mol^{-1}$ in intensively managed grasslands of the North Atlantic (Cabauw, the Netherlands), with a mean value of $\alpha_{nonfor} = 33.3$ $mmol \cdot mol^{-1}$ and a standard deviation of $s_{nonfor} = 14.2$ $mmol \cdot mol^{-1}$. The lower 10% quantile of the α values in the sample (5–17 $mmol \cdot mol^{-1}$) included extensively managed arid and semiarid grasslands and shrublands (Karrykul, Cottonwood, Karnap, Audubon, Lethbridge, Kherlenbayan-Ulaan, Tojal, and Fort Peck), while the upper 10% quantile (50–75 $mmol \cdot mol^{-1}$) encompassed intensively managed grasslands (Cabauw, Carlow, Neustift, Easter Bush, Oensingen, Lille Valby, Grillenburg, Haller), extensively managed grasslands under favorable weather conditions (Laqueuille-extensive, Rigi-Seebodenalp, Jornada),

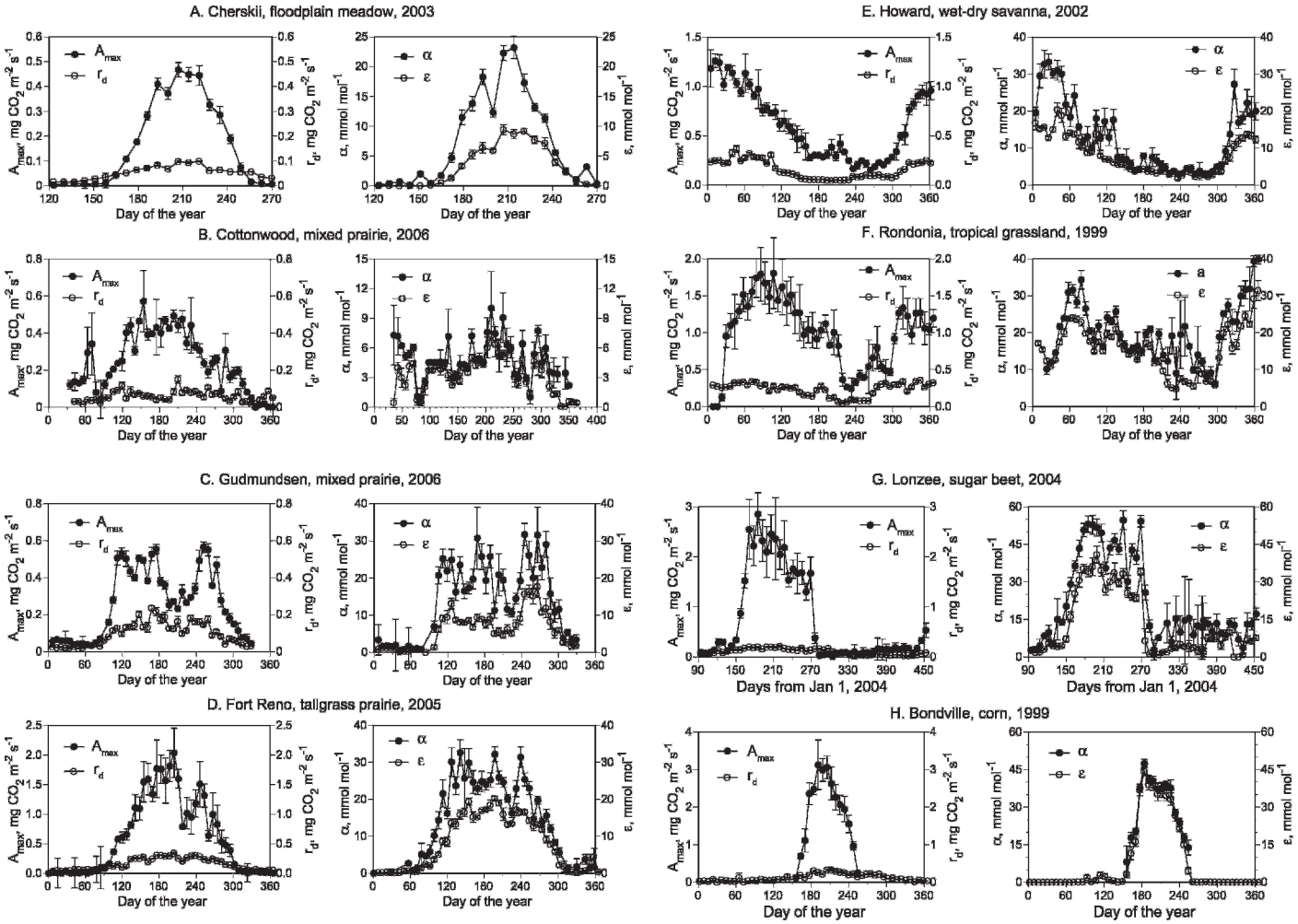

Figure 6. Seasonal dynamics of light-response parameters: maximum photosynthesis, A_{max}, daytime ecosystem respiration, r_d, quantum yield, α, and gross ecological light-use efficiency, ε, in selected nonforest ecosystems: **A**, floodplain meadow, Cherskii, 2003; **B**, mixed prairie, Cottonwood, 2006; **C**, mixed prairie, Gudmundsen Ranch, 2006; **D**, tallgrass prairie, Fort Reno, 2005; **E**, wet-dry savanna, Howard, 2002; **F**, tropical grassland, Rondonia, 1999; **G**, sugar beet, Lonzee, 2004; **H**, maize crop, Bondville, 1999.

and intensive agricultural crops (Lonzee). Interestingly, most productive crop sites, characterized by the highest A_{max} and $P_{g,max}$ values, were not included in the upper 10% quantum yield quantile, although they often were parceled into the upper 20% quantum yield quantile.

Besides examining scatter plots for the pooled data set, understanding relationships among parameters within a particular ecosystem is of interest. Presently, only a subset of extensively managed grasslands had scatter diagrams that exhibited pronounced patterns of covariation (Fig. 5).

In evaluating estimates of quantum yield, our maximum estimate of 75 $mmol \cdot mol^{-1}$ was only two-thirds of the theoretical maximum of quantum efficiency of gross photosynthesis estimated by Good and Bell (1980; 110 $mmol \cdot mol^{-1}$). We compared our nonforest estimates with those reviewed by Ruimy et al. (1995) from which we estimated a mean $\overline{\alpha}_{forest} = 37$ $mmol \cdot mol^{-1}$ with a standard deviation of $s_{forest} = 17$ $mmol \cdot mol^{-1}$, excluding data in Ruimy et al. 1995 with α values greater than the theoretical maximum of quantum efficiency after Good and Bell (1980). We found that quantum efficiency of non-forest ecosystems was not statistically different from forests. In fact, $\alpha_{max,nonforest}$ estimated for intensively managed Cabauw grassland in the Netherlands (75 $mmol \cdot mol^{-1}$) was numerically higher, but statistically not significantly different from the maximum quantum efficiency determined for the chestnut coppice near Paris, France ($\alpha_{max,forest} = 73$ $mmol \cdot mol^{-1}$; Mordacq et al. 1991).

The values of maximum average weekly gross photosynthesis, A_{max}, for nonforest sites of the world (Fig. 4A) ranged from 0.2 mg $CO_2 \cdot m^{-2} \cdot s^{-1}$ (Fort Peck mixed prairie during a drought year) to 3.4 mg $CO_2 \cdot m^{-2} \cdot s^{-1}$ (Mead, irrigated continuous maize). The lower 10% quantile (0.2–0.36 mg $CO_2 \cdot m^{-2} \cdot s^{-1}$) included Fort Peck, Dubois, Miles City, Kherlenbayan-Ulaan, Xilinhot, Karrykul, Kubuqi, Burns, and Karnap, and the upper 10% quantile (2–3.4 mg $CO_2 \cdot m^{-2} \cdot s^{-1}$) included intensive crops (Mead, Bondville, Lonzee, Ames), intensively managed grasslands (Cabauw, Carlow, Lille Valby), and tallgrass prairies (Shidler, Fort Reno). The mean photosynthetic capacity of nonforest ecosystems (1.2 mg $CO_2 \cdot m^{-2} \cdot s^{-1}$, SD = 0.68 mg $CO_2 \cdot m^{-2} \cdot s^{-1}$) lies at the upper end of the mean A_{max} range for different forest types from eddy covariance estimates (0.66 mg $CO_2 \cdot m^{-2} \cdot s^{-1}$

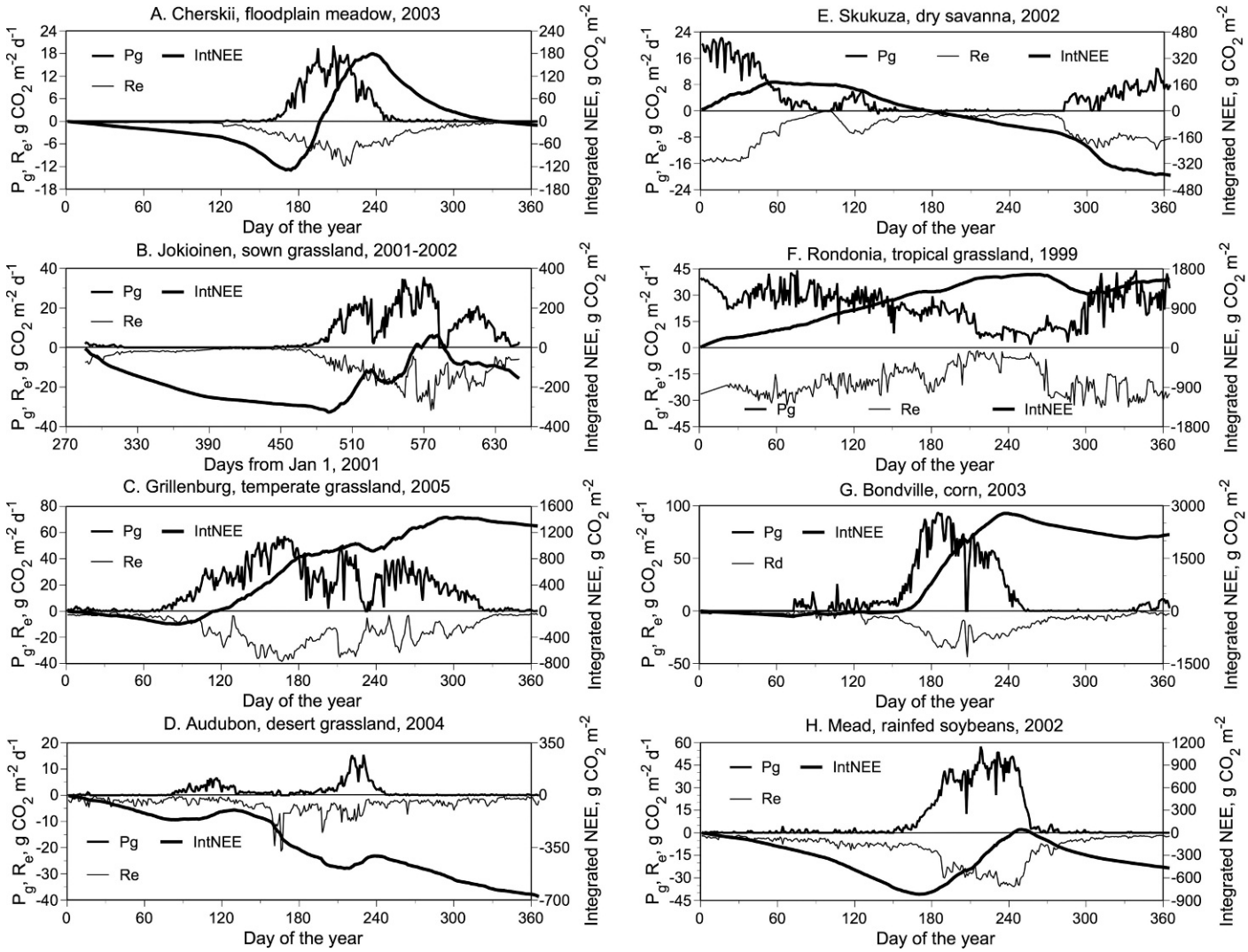

Figure 7. Seasonal dynamics and annual budgets of gross primary productivity, $P_g(t)$, total ecosystem respiration, $R_e(t)$, and integrated net ecosystem CO_2 exchange, IntNEE(t), for selected nonforest sites and years: **A**, floodplain meadow, Cherskii, 2003; **B**, sown northern temperate grassland, Jokioinen, 2001–2002; **C**, temperate grassland, Grillenburg, 2005; **D**, desert grassland, Audubon Ranch, 2004; **E**, dry savanna, Skukuza, 2002; **F**, tropical grassland, Rondonia, 1999; **G**, maize crop, Bondville, 2003; **H**, soybean crop, Mead, 2002.

to 1.3 mg $CO_2 \cdot m^{-2} \cdot s^{-1}$, mean = 0.97 mg $CO_2 \cdot m^{-2} \cdot s^{-1}$; Falge et al. 2002; Funk and Lerdau 2004). At the same time, the highest A_{max} value for nonforest ecosystems found in intensive maize cultures of the midwestern United States (3.4 mg $CO_2 \cdot m^{-2} \cdot s^{-1}$) were substantially higher than A_{max} = 2.64 mg $CO_2 \cdot m^{-2} \cdot s^{-1}$ estimated from data by Jarvis (1994) for a Sitka spruce culture in Scotland.

The values of daytime ecosystem respiration rate (r_d) in all ecosystems were substantially lower than corresponding A_{max} values (cf. Fig. 6, left), but varied substantially among ecosystem types (Fig. 4B) with maximum weekly average r_d ranging an order of magnitude from 0.04 mg $CO_2 \cdot m^{-2} \cdot s^{-1}$ (Burns, drought year) to 0.45 mg $CO_2 \cdot m^{-2} \cdot s^{-1}$ (Ames, Neustift, warm and wet years). The lower 10% quantile of maximum weekly r_d values included arid and semiarid grasslands and shrublands (Burns, Karnap, Kherlenbayan-Ulaan, Karrykul, Cottonwood, Burns, Dubois, Kubuqi) and tundra (Barrow). The upper 10% quantile of r_d distribution was represented by intensively managed grasslands (Neustift, Cabauw, Carlow, Oensingen, Lille Valby, Easter Bush, Haller), intensive crops (Ames, Mead), tallgrass prairies (Shidler, Rannels Ranch), and a semidesert grassland in a year with exceptionally high precipitation (Jornada).

The weekly maxima of the coefficient of gross ecological light-use efficiency, ε, observed in this study ranged from 3 to 59 mmol · mol^{-1} (mean 22, standard deviation 12.4 mmol · mol^{-1}) and were lower than the weekly maxima of apparent quantum yield, α (Fig. 6, right). For some ecosystems, particularly for agricultural C_4 crops and tropical grasslands dominated by C_4 species, ε values were not considerably lower than α (e.g., see Figs. 6E, 6F, and 6H, right). This is a direct result of relatively high values of the convexity coefficient of the light curves of C_4 species; for the case where θ = 1, the values of α and ε become equal, provided input radiation levels remain within the range of linear light response.

In C_3 communities characterized by low convexity values (θ = 0 in the extreme case of rectangular hyperbolic light response), ecological light-use efficiency remains substantially

Table 4. Statistical characteristics of annual gross primary production (GPP), total ecosystem respiration (RE), and net ecosystem exchange (NEE) for major groups within nonforest terrestrial ecosystems.

Statistical characteristics	Ecosystem group				
	Grasslands extensively managed	Grasslands intensively managed	Shrublands and savanna	Wetlands	Croplands
GPP ($g\ CO_2 \cdot m^{-2} \cdot yr^{-1}$)					
No. of site-years	173	40	28	48	66
Mean	565	6 014	2 949	2 328	4 521
SD	1 698	1 133	1 950	1 836	1 365
Min.	95	3 141	645	749	1 376
Max.	8 600	7 720	6 836	5 643	6 774
RE ($g\ CO_2 \cdot m^{-2} \cdot yr^{-1}$)					
No. of site-years	163	40	27	18	66
Mean	2 370	5 296	2 537	1 824	3 588
SD	1 469	1 040	1 396	1 373	909
Min.	112	3 186	756	665	1 052
Max.	7021	7 880	5 094	4 751	5 905
NEE ($g\ CO_2 \cdot m^{-2} \cdot yr^{-1}$)					
No. of site-years	163	40	27	18	66
Mean	255	700	493	504	933
SD	521	717	740	719	814
Min.	− 1 342	− 961	− 585	− 40	− 770
Max.	1 762	2 394	2 254	2 226	2 382

lower than quantum yield (Fig. 6A, right). The lower 10% quantile of light-use efficiency values ε (2.6–6.4 $mmol \cdot mol^{-1}$) includes deserts, desert and dry-steppe grasslands, shortgrass and sagebrush steppes, mixed prairies, California grasslands and chaparral, and tundra (Karrykul, Karnap, Audubon Ranch, Kendall, Xilinhot, Central Plains Experimental Range, Fort Peck, Cottonwood, Burns, Kubuqi, Kherlenbayan-Ulaan, Sky Oaks, Barrow, Atqasuk, Ivotuk). The upper 10% quantile of the ε values (40–59 $mmol \cdot mol^{-1}$) mostly included high-yield crops (Risbyholm, Langerak, Molenweg, Mead, Bondville, Oensingen, Gebesee, Lonzee, Batavia) as well as highly productive managed grasslands (Carlow, Lille Valby, Oensingen, Neustift).

To compare ε_{max} estimates for forest and nonforest ecosystems, we calculated average weekly values of light-use efficiency for the 12 most productive forest ecosystems in the FLUXNET La Thuile database. These 12 ε_{max} values ranged between 29.1 and 47.7 $mmol \cdot mol^{-1}$, with the highest value found in the 2001 data set for the Duke loblolly pine forest (North Carolina), which is less than $\varepsilon_{max} = 59\ mmol \cdot mol^{-1}$ for a high-yield crop (also, see Table 5 for $P_{g,max}$ comparison of forests and nonforest ecosystems). Thus, the light-use efficiency data agreed with observations presented earlier in this section that the values of maximum apparent quantum yield in nonforest ecosystems (particularly, intensively managed grasslands) were comparable and sometimes higher than those for forest ecosystems.

Parameter Interrelations

As expected, numerical values of light-response parameters among various ecosystems did not vary independently of each other, but demonstrated patterns of correlation (Figs. 4 and 5). Our results for this extensive data set agreed with those of earlier studies with smaller subsets of flux-tower data, suggesting that the plateau parameter of gross photosynthesis, A_{max}, was a good predictor for other light-response parameters, including quantum yield, α, ecosystem respiration rate, r_d, and light-use efficiency, ε (Gilmanov et al. 2007; Owen et al. 2007). Baldocchi and Xu (2005) found that A_{max} was a good predictor for another photosynthetic parameter, the maximum rate of carboxylation ($V_{c,max}$). In previous studies, mostly linear relationships were observed between A_{max} and other parameters; however, the wider range of parameter variations in our data set revealed a number of distinct nonlinearities. For example, a power-law relationship $\alpha = 30.36(A_{max})^{0.55}$ with R^2 value of 0.55 was obtained for the relationship between apparent quantum yield and maximum photosynthesis (Fig. 4A). The better fit of the nonlinear (with power exponent < 1) description of the $\alpha(A_{max})$ relationship compared to the simple linear model was demonstrated by the fact that the nonlinear model exhibited a decrease in α with decreasing A_{max} as the latter approached 0, while the linear model predicted an unrealistic α_0 value of $\sim 15\ mmol \cdot mol^{-1}$ even when A_{max} approached 0.

Daytime ecosystem respiration (r_d) also demonstrated a power law relationship with A_{max} described as $r_d = 0.22(A_{max})^{0.71}$ with $R^2 = 0.69$ (Fig. 5B). In this case, the linear model also provided a reasonable fit to the data ($R^2 = 0.67$), though its applicability to the region of low A_{max} values was limited by an unrealistically large intercept of $r_d = 0.09\ mg\ CO_2 \cdot m^{-2} \cdot s^{-1}$ as A_{max} approached 0. From the patterns of data points in Figures 5C and 5D, the relationships between ecological light-use efficiency, maximum daily gross photosynthesis, and L_{max} may be approximated by both the linear and the power-law equations, though the latter provided better fit in the lower range of A_{max} and L_{max}.

Maximum leaf area (L_{max}) and/or maximum aboveground green biomass (G_{max}) was not available for all flux sites. With the limited data available (Figs. 5F and 5H), we established nonlinear power law (with exponent coefficient < 1) dependence of maximum photosynthesis parameters (A_{max}, $P_{g,max}$) and the standard morphometric characteristics such as maximum aboveground biomass, G_{max}, and maximum leaf area index, L_{max} (Figs. 5F and 5H).

Seasonal Patterns of Parameter Dynamics

The light-response parameters evaluated from flux-tower measurement data sets represented not only physiological characteristics (which also change through time with phenology and environmental conditions) but also ecosystem-scale attributes such as aboveground biomass, leaf-area index, and others. As a result, such parameters exhibited pronounced variation in magnitude during the year. Seasonal changes of these parameters, though specific for particular sites and years, exhibited general patterns revealed in time plots of parameter values aggregated at the weekly time step (Fig. 6). Pronounced seasonal dynamics of light-response parameters for cold and temperate environments were closely related to radiation and temperature (Figs. 6A and 6D); however, under arid conditions they were closely associated with fluctuations in precipitation (Figs. 6E and 6F). This climatically driven unimodal pattern of seasonal parameter change was particularly pronounced in species-poor ecosystems or monocultures with a relatively narrow production period, be that a floodplain meadow in the tundra zone (Fig. 6A) or agricultural crops (Figs. 6G and 6H). In ecosystems with a higher species diversity and broader production period (up to year-round production under tropical conditions), the general seasonal pattern of parameter dynamics was compounded by additional fluctuations that reflected different reactions of various species groups (e.g., cool and warm-season grasses) to weather variability and management regime (grazing, mowing) during various parts of the year (Figs. 6B–6D). These data may help to explain difficulties experienced by those attempting to simulate year-round dynamics of gross primary productivity and light-response parameters by modification of the hypothetical maximum parameter value by factors–multipliers that describe effects of various drivers such as radiation, temperature, moisture, etc. (cf. Monteith 1972; Ciais et al. 2001).

Seasonal Dynamics and Annual Budgets of GPP, RE, and NEE

Depending on a number of external (e.g., radiation, temperature, precipitation) and internal (e.g., leaf area, phenological state, water and nutrient supply) ecological factors, the functions of gross primary productivity ($P_g[t]$), and total ecosystem respiration ($R_e[t]$) demonstrated pronounced temporal dynamics during the year. This was exemplified by measurement-based estimates of $P_g(t)$ and $R_e(t)$ (Fig. 7). The curve of integrated net ecosystem exchange (IntNEE[t]) was much smoother, and its value at the end of the year (NEE) provided a summary of ecosystem CO_2 budget.

Data from the analyzed data sets demonstrated a large variety of seasonal patterns of productivity and respiration dynamics, with some of the typical curves illustrated in Figure 7. Three major seasonal patterns of the cumulative

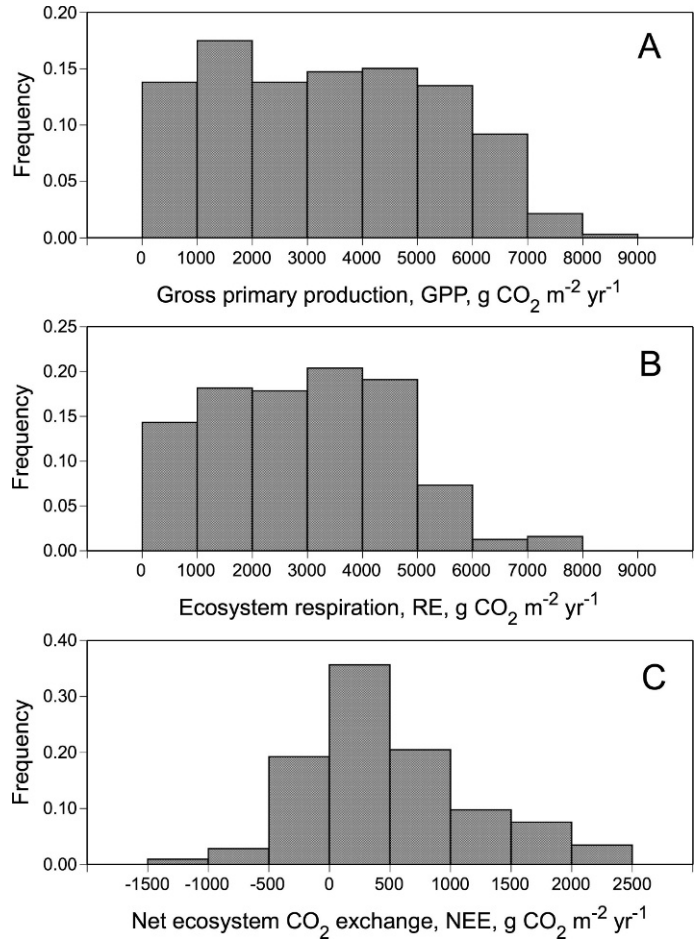

Figure 8. Frequency distributions of **A**, gross primary production (GPP); **B**, ecosystem respiration (RE); and **C**, net ecosystem CO_2 exchange (NEE) estimates in the pooled set site-years from nonforest flux-tower sites.

NEE curve were evident: 1) equilibrium (S-shaped), 2) permanent accumulation, and 3) permanent release of carbon. The equilibrium pattern (1) characterizing nonharvested ecosystems with marked seasonality of primary productivity was exemplified by data from a floodplain tundra meadow at Cherskii in the Far northeast of Russia (Fig. 7A). With the period of decomposition activity (May–September) completely encompassing the production period (June–August) and with maximum decomposition lagging behind maximum production, the curve of cumulative NEE assumed a characteristic S-shaped form with the net annual ecosystem CO_2 exchange near zero. The accumulative pattern was described by the more or less monotonous accumulation of net ecosystem production in ecosystems with a period of marked domination of production compared to decomposition processes observed in both grassland (Fig. 7F) and cropland ecosystems (Fig. 7G). The third pattern of nearly permanent domination of respiratory efflux over assimilatory uptake resulting in significant net loss of carbon dioxide from the ecosystem at the end of the year was exemplified by measurements at the Audubon (AZ) desert grassland on a high carbonate soil (Fig. 7D; cf. Emmerich 2003). These three major patterns were accompanied by a variety of intermediate variants with local maxima and minima

Table 5. Maximum values of daytime gross primary productivity, $P_{g,max}$, and annual net primary production, GPP, estimated for nonforest and forest flux-tower sites.

Site	Year	$P_{g,max}$ g $CO_2 \cdot m^{-2} \cdot d^{-1}$	Site	Year	GPP g $CO_2 \cdot m^{-2} \cdot yr^{-1}$
Grasslands extensively managed					
Jornada, NM, USA	2000	63.1	Rondonia, Brazil	1999	8 600
Rannels Ranch, KS, USA	1998	60.8	Goodwin Creek, MS, USA	2004	6 391
Batavia Prairie Site, IL, USA	2006	59.9	Grillenburg, Germany	2005	6 299
Grillenburg, Germany	2005	57.34	Duke grassland, NC, USA	2003	6 039
Monte Bondone, Italy	2006	56.9	Laqueuille, France, extensive	2006	5 943
Shidler, OK, USA	1999	56.9	Neal Smith, IA, USA	2005	5 756
Temple, TX, USA	1999	56.2	Batavia Prairie Site, IL, USA	2006	5 435
Oensingen, Switzerland	2003	53.6	Oensingen, Switzerland	2003	5 326
Neal Smith, IA, USA	2005	52.7	Laqueuille, France, extensive	2004	5 322
Laqueuille, France, extensive	2004	51.7	Rigi-Seebodenalp, Switzerland	2003	5 320
Goodwin Creek, MS, USA	2003	51.4	Shidler, OK, USA	1997	5 208
Amplero, Italy	2004	48.1	Monte Bondone, Italy	2006	5 168
Grasslands intensively managed					
Cabauw-extension, The Netherlands	2005	76.3	Oensingen, Switzerland	2004	7 720
Neustift, Austria	2004	76.2	Neustift, Austria	2006	7 415
Easter Bush, United Kingdom	2003	63.6	Dripsey-grass, Ireland	2004	7 388
Oensingen, Switzerland	2004	63.5	Haastrecht, The Netherlands	2003	7 267
Lille Valby, Denmark	2006	63.4	Lille Valby, Denmark	2004	6 873
Haastrect, Netherlands	2003	63.1	Laqueuille, France, intensive	2004	6 838
Laqueuille, France, intensive	2006	59.0	Carlow-grassland, Ireland	2003	6 807
Carlow-grassland, Ireland	2003	57.9	Easter Bush, United Kingdom	2003	6 793
Haarweg, The Netherlands	2002	57.5	Cabauw-extension, The Netherlands	2005	6 785
Dripsey-grass, Ireland	2003	54.7	Haarweg, The Netherlands	2002	5 915
Lacombe, Alberta, Canada	2003	53	Hegyhátsál, Hungary	1999	5 867
Haller, State College, PA, USA	2004	52.2	Cabauw, The Netherlands	2004	5 837
Shrubs and savannas					
Howard Springs, Australia	2005	54.2	Sao Paulo cerrado, Brazil	2002	6 836
Sao Paulo cerrado, Brazil	2002	42.7	Howard Springs, Australia	2002	5 874
Tonzi Ranch, California	2005	38.6	Skukuza, South Africa	2001	3 947
Skukuza, South Africa	2001	34.6	Tonzi Ranch, CA, USA	2005	3 837
Tonzi Ranch, California	2003	34.1	Sky Oaks Old stand, CA, USA	1997	2 682
Sky Oaks Young stand, CA, USA	1998	22.7	Sky Oaks Young stand, CA, USA	1998	2 021
Sky Oaks Old stand, CA, USA	1997	21.0	Skukuza, South Africa	2003	1 873
Santa Rita mesquite, AZ, USA	2005	19.8	Santa Rita mesquite, AZ, USA	2005	1 125
Kubuqi, shrubland, China	2006	12.8	Kubuqi, shrubland, China	2006	1 021
Karrykul, Turkmenistan	2000	7.79	Karrykul, Turkmenistan	2000	769
Wetlands					
Dongtan marsh-2, China	2005	70.1	Dongtan marsh-2, China	2005	5 643
CzechWet, Czech Republic	2006	56.9	CzechWet, Czech Republic	2006	5 368
Dongtan marsh-1, China	2005	51.9	Dongtan marsh-1, China	2005	5 150
Dongtan marsh-3, China	2005	43.3	Tadham Moore, United Kingdom	2001	4 767
Tadham Moore, United Kingdom	2001	41.1	Dongtan marsh-3, China	2005	3 662
PolWet, Poland	2005	41.1	PolWet, Poland	2005	3 393
Cherskii, Russia	2003	20.1	Siikaneva, Finland	2005	1 359
Kaamanen wetland, Finland	2005	19.8	Kaamanen wetland, Finland	2005	1 210
Siikaneva, Finland	2004	19.8	Cherskii, Russia	2003	834
Croplands					
Mead, maize rot. irrigated, NE, USA	2001	116.1	Langerak, The Netherlands	2005	6 774
Mead, maize cont. irrigated, NE, USA	2001	107.8	Mead, rot. maize irrigated, NE, USA	2003	6 720
Bondville, maize, IL, USA	1999	99.9	Borgo Cioffi-crop, Italy	2005	6 513

Table 5. Continued.

Site	Year	$P_{g,max}$ g $CO_2 \cdot m^{-2} \cdot d^{-1}$	Site	Year	GPP g $CO_2 \cdot m^{-2} \cdot yr^{-1}$
Batavia-agro, IL, USA	2006	99.0	Mead, cont. maize irrigated, NE, USA	2001	6 437
Bondville, maize, IL, USA	1999	94.1	Borgo Cioffi-crop, Italy	2006	6 393
Borgo Cioffi-crop, Italy	2006	93.1	Mead, maize rotation irrigated	2001	6 316
Mead, maize rainfed, NE, USA	2003	87.6	Lonzee, Belgium, sugar beet	2005	6 313
Langerak-crop, France	2006	87.5	Oensingen-crop, Switzerland	2005	6 295
Bondville-companion, IL, USA	2006	83.03	Mead maize rainfed, NE, USA	2001	5 834
Grignon-crop, France	2005	81.3	Bondville, maize, IL, USA	1999	5 602
Lonzee, winter wheat, Belgium	2005	80.5	Bondville, soybeans, IL, USA	2005	5 582
Bondville, soybeans, IL, USA	2005	80.1	Risbyholm, Denmark, crop	2004	5 525
Forests and plantations					
Duke Forest Loblolly Pine, NC, USA	2001	99.0	French Guyana	2004	14 339
Campbell River, British Columbia, Canada	1998	86.6	Vanuatu - CocoFlux	2002	13 057
Hampshire Forest, United Kingdom	2004	73.9	Rondonia forest, Brazil	2002	12 727
Duke Forest Loblolly Pine	2005	69.0	Palangkaraya, Indonesia	2003	12 236
Vanuatu - CocoFlux	2003	68.2	Santarem km67 primary forest, Brazil	2003	11 703
Duke Forest Hardwood, NC, USA	2003	67.6	Caxiuana Forest-Almeirim, Brasil	2002	11 436
French Guyana	2005	64.21	Santarem km67 primary forest, Brazil	2002	11 271
Rondonia forest, Brazil	2002	60.8	Loblolly Pine plantation, NC, USA	2006	10 173
Campbell River, British Columbia, Canada	2000	60.1	Donaldson Slash Pine Plantation, FL, USA	1999	9 249
Loblolly Pine plantation, NC, USA	2006	59.7	Campbell River, British Columbia, Canada	2005	9 162
Duke Forest Hardwood, NC, USA	2004	57.5	Duke Forest Loblolly Pine, NC, USA	2002	9 067
Donaldson Slash Pine Plantation, FL, USA	1999	54.6	Duke Forest Hardwood, NC, USA	2003	8 892

of the IntNEE(t) curve reflecting weather fluctuations and harvesting, which finally led to either net uptake (Fig. 7C) or net loss of carbon from the ecosystem (Figs. 7B, 7E, and 7H). Hendricks et al. (2007) described a case were S-shaped IntNEE dynamics was combined with significant net accumulation of carbon in a peat meadow ecosystem.

Year-round integration of the $P_g(t)$, $R_e(t)$, and $F_c(t)$ curves provided estimates of annual GPP, RE, and NEE totals for all the site-years in this study. These data stratified by major ecosystem groups (extensively and intensively managed grasslands, shrublands and savanna, wetlands, and croplands) are summarized in Table 4. The highest mean gross primary production (6 014 g $CO_2 \cdot m^{-2} \cdot yr^{-1}$) and ecosystem respiration (5 296 g $CO_2 \cdot m^{-2} \cdot yr^{-1}$) were achieved in intensively managed grasslands. Not surprisingly, the highest mean annual net ecosystem CO_2 exchange (933 g $CO_2 \cdot m^{-2} \cdot yr^{-1}$) was found in croplands.

To supplement these basic statistical characteristics, Figure 8 shows the distributions of GPP, RE, and NEE values in the pooled data set of estimates from all site-years in the database. They showed that the GPP and RE values in our sample varied widely (95–8 600 g $CO_2 \cdot m^{-2} \cdot yr^{-1}$ for gross production and 112–7 880 g $CO_2 \cdot m^{-2} \cdot yr^{-1}$ for respiration), with GPP and RE values fairly well distributed across their ranges (Figs. 8A and 8B). Net CO_2 exchange values, however, concentrated between − 1 342 g $CO_2 \cdot m^{-2} \cdot yr^{-1}$ and 2 394 g $CO_2 \cdot m^{-2} \cdot yr^{-1}$ and had a distinctly unimodal distribution (Fig. 8C). The average NEE value for our sample of 316 nonforest ecosystems was 485 g $CO_2 \cdot m^{-2} \cdot yr^{-1}$ (SD = 696 g $CO_2 \cdot m^{-2} \cdot yr^{-1}$). Comparing these statistics with the mean (671 g $CO_2 \cdot m^{-2} \cdot yr^{-1}$) and standard deviation (988 g $CO_2 \cdot m^{-2} \cdot yr^{-1}$) of published NEE values for 506 site years from flux towers worldwide (Baldocchi 2008b), we did not detect a difference between the two NEE averages at the 1% level of significance. The higher mean NEE value for Baldocchi's sample can be explained by the number of growing forest sites with high NEE included in the sample, while the WORLDGRASSAGRIFLUX data set included mostly non-forest sites (with occasional near-climax shrubland and savanna ecosystems).

In the context of comparing basic parameters of the carbon cycle, it is particularly interesting to identify maximum rates of photosynthetic CO_2 assimilation in various ecosystems. For this purpose, we compiled data of the 12 (or maximum available) site-years with maximum values of daily photosynthesis, $P_{g,max}$, and 12 (or maximum available) site-years with maximum annual GPP for our five types of nonforest ecosystems and for the forest sites represented in the most recent FLUXNET database (Table 5). For annual GPP, forest ecosystems achieved the highest estimates of photosynthetic CO_2 uptake, with a maximum GPP = 14 339 g $CO_2 \cdot m^{-2} \cdot yr^{-1}$ for a tropical forest in French Guyana (Table 5) compared to a maximum GPP = 8 600 g $CO_2 \cdot m^{-2} \cdot yr^{-1}$ for a tropical grassland in Rondonia, Brazil (Table 5). In contrast, maximum daily rates of photosynthetic uptake were found not in forests, but in the intensive crops of the midwestern United States, with $P_{g,max}$ = 116 g $CO_2 \cdot m^{-2} \cdot d^{-1}$ estimated for

irrigated maize in a maize–soybean rotation (Mead, NE) in 2001 (Table 5). These data clearly demonstrate that even in nonforest ecosystems such as shrublands and savanna, maximum rates of gross photosynthetic assimilation (50–76 g $CO_2 \cdot m^{-2} \cdot d^{-1}$) were quite comparable to those of the most productive forests (55–99 g $CO_2 \cdot m^{-2} \cdot d^{-1}$). A major reason why annual GPP in forests is typically higher than nonforested ecosystems is the length of production period. In tropical forests, production may encompass the whole year, whereas in most nonforest ecosystems production is temporally limited by temperature and water availability.

Source/Sink Activity of Nonforest Ecosystems

The data on annual budgets of production, respiration, and net CO_2 exchange of nonforest ecosystems obtained in our study allowed a quantitative evaluation of important questions concerning the magnitude and significance of their source or sink activity. Since Odum (1956; see also Baldocchi 2008b), a convenient way to visualize the net CO_2 budget of ecosystems for comparative purposes has been the use of RE vs. GPP scatter diagrams and comparison of the distribution of data points with respect to the 1:1 diagonal. Points below the diagonal correspond to sinks ($GPP > RE$, $NEE > 0$), whereas points above the diagonal describe sources of CO_2 ($GPP < RE$, $NEE < 0$).

An Odum plot for the whole nonforest data set used in our study (Fig. 9) demonstrated that for four out of every five site-years, gross production was higher than ecosystem respiration, indicating net ecosystem sink activity. Stratification of the data with respect to ecosystem type (Fig. 10) showed that there were considerably more years with net CO_2 uptake than release for all types of nonforest ecosystems in our database. However, years with net source activity occasionally occurred over the study period in all ecosystems, except wetlands. It should be recognized that in managed nonforest ecosystems (as in managed forests), part of the carbon accumulation occurs in pools that may be exported off-site (as crop and forage harvest in nonforest ecosystems or as timber in forests).

The distributions of NEE for different ecosystems presented in Figure 11 provide a more detailed description of the matter. Source-type activity more frequently occurred in extensively managed grasslands, shrublands/savanna, and croplands than in intensively managed grasslands and wetlands. As a rule, source-type activity was associated with years of drought, excessive grazing and hay mowing, fire, high organic matter content of soils (e.g., grasslands on peat) or high $CaCO_3$ stocks in the soil profile, and transitional successional status of the ecosystem (e.g., grasslands of previously forested soils; Meyers 2001; Emmerich 2003; Suyker et al. 2003; Novick et al. 2004; Jacobs et al. 2007). For agroecosystems, source activity was reported for crops such as soybeans, which typically involve intensive soil preparation and relatively short active growth periods (Baker and Griffis 2005). However, it should be emphasized that for the majority of ecosystems in our study, CO_2 sink activity was frequently observed (from the atmospheric point of view), with the highest net carbon uptakes in intensively managed grasslands and cropland ecosystems, which are harvested once or several times each year and lead to off-site decomposition of the harvested products (Fig. 11, Table 4). In the past, a number of authors reported data that documented positive NEE values for grasslands and croplands (Svejcar et al. 1997; Dugas et al. 1999; Frank et al. 2001; Mielnick et al. 2001; Barcza et al. 2003; Suyker et al. 2003; Anthoni et al. 2004; Gilmanov et al. 2004; Xu and Baldocchi 2004; Gilmanov et al. 2005; Bernacchi et al. 2006; Gilmanov et al. 2006; Jaksic et al. 2006; Moureaux et al. 2006; Jacobs et al. 2007; Svejcar et al. 2008; Aubinet et al. 2009; Béziat et al. 2009). In our present analysis, we found predominantly positive annual NEE in managed grasslands and croplands based on a large number of geographically distributed flux monitoring stations from a variety of networks (Fig. 8C).

These observations contradict the conclusions of the first state of the carbon cycle report (SOCCR; King et al. 2007) and some earlier reports (e.g., Reicosky 1997; Smith and Falloon 2005), which assumed net source or neutral activity of agricultural ecosystems. These authors considered carbon stock changes, not the balance of CO_2 fluxes exchanged with the atmosphere. In managed nonforest ecosystems, annual exports of organic matter by harvest imply that carbon storage does not vary in proportion to net balance of CO_2 fluxes exchanged with atmosphere (Soussana et al. 2007). Our analysis shows a preponderance of data indicating predominantly positive net ecosystem CO_2 exchange in grasslands and agroecosystems (Table 4, Figs. 8–11). Positive values of NEE based on CO_2 flux measurements, however, do not necessarily mean there is an accumulation of carbon in the ecosystem, which may be lost as methane (Hendricks et al. 2007), or removed in nongaseous form with harvest or erosion. Given the role of harvest and anthropogenic management, results from our analysis indicate that the ability of managed agroecosystems and grasslands to serve as net sinks of CO_2 from the atmosphere may be substantial, depending on the ultimate fate of the harvested biomass.

The need to recognize the sink activity of many grassland and agroecosystems to better understand the cycling of carbon at the landscape and regional level may be illustrated by imagining the vector field describing the movement of CO_2 from the atmosphere to the ecosystem and back using a rather detailed space-time scale (e.g., 250-m 7-d MODIS). The CO_2-NEE data (and methane and other gaseous forms of carbon exchange with the atmosphere, where measured) show that for many nonforest ecosystems, a particular pixel will have more arrows coming in than going out. Harvesting, erosion, and other forms of lateral transport of carbon in nongaseous form means that carbon is moved to other locations. Although the carbon eventually may be returned to the atmosphere in gaseous form, this release may occur from other pixels, often located far away from the original pixel into which the CO_2 was assimilated. An independent validation of our conclusion about the predominant sink activity of managed grassland and agricultural ecosystems is provided by patterns of net CO_2 exchange generated by the National Oceanic and Atmospheric Administration's CarbonTracker system based on precise measurements and modeling of atmospheric CO_2 mole fractions (Peters et al. 2007; CarbonTracker 2009). Their map of the annual CO_2 exchange for North America (Peters et al. 2007, fig. 1) shows significant carbon uptake in the Great Plains and the Midwest megaregions dominated by grassland and agroecosystems with the summary CO_2 uptake of grassland and crop areas being higher than that of the largest North American sink, coniferous forests (Peters et al. 2007, fig. 2).

The positive NEE values identified in the present study should stimulate efforts to combine flux measurements with full organic matter accounting, which so far has been implemented at only a few sites (Anthoni et al. 2004; Verma et al. 2005; Bernacchi et al. 2006; Amman et al. 2007; Soussana et al. 2007; Aubinet et al. 2009). In this context, it is also appropriate to consider the argument of Körner (2003) regarding the critical significance of the representativeness of flux-tower data sets and the "slow in, fast out" role of the biosphere in the dynamics of the carbon cycle. Recognizing the relevance of Körner's arguments to the situation in the early 2000s, it should be emphasized that, at least with regard to nonforest ecosystems, the present set of flux-tower sites that were analyzed in our study includes a wide range of sites with a large diversity of climatic conditions and management regimes. Therefore, data analyzed in the present study are much less biased toward highly productive ecosystems; however, southern hemisphere, south Asian, and African ecosystems tend to be underrepresented in the present analysis (Fig. 1).

Ecosystem-Scale Production and Respiration in Relation to Major Ecological Factors

Relationships of production and decomposition to major ecological factors attracted the attention of ecologists and geographers of the 20th century (Weaver 1924; Walter 1939; Budyko and Efimova 1968; Rosenzweig 1968; Lieth 1975) and were later approached under the framework of dynamic global vegetation models and related models (e.g., Woodward et al. 2001; Cramer et al. 2001). Presently, these problems are back in the focus of ecosystem and regional and global ecology, not only because of the recognition of their relevance to global climatic change, but also because today, for the first time, measurement-based quantitative estimates of gross productivity and total ecosystem respiration are readily available through processing of net CO_2 exchange measurements at flux-tower sites (Aubinet et al. 2000; Baldocchi et al. 2001; Yaun et al. 2007; Zhang et al. 2007; Skinner et al. 2008).

Besides radiation and temperature, which are taken into account by the light–temperature-response function method, the next most important factor influencing ecosystem productivity and respiration is water (e.g., Slatyer 1967; Boyer 1982). Though water content or water potential of topsoil horizons are the most desirable predictors in production and decomposition modeling efforts, such data are not yet readily available for many flux-tower stations, making it necessary to use available precipitation data.

Both theory and empirical data indicate nonlinear relationships between photosynthesis, productivity, and decomposition rates and water content and/or water potential (Denmead and Shaw 1962; Wildung et al. 1975; Singh et al. 1980; Eastin and Sullivan 1984; Mielnick and Dugas 2000). In contrast, observations of the linear response of productivity in certain ecosystem types occasionally appear in the literature (Walter 1939; Le Houèrou and Hoste 1977; Sala et al. 1988). Our data allow a fresh look at this old problem by using new ecosystem-scale estimates of GPP and RE values in relation to atmospheric precipitation (PCPN; Fig. 12). Within the whole data set, we found that the subsets of extensively managed grasslands, intensively managed grasslands, and shrublands–savanna exhibit patterns of the relationship of GPP and RE to precipitation and the dryness index. The data for wetlands and croplands, however, did not produce recognizable patterns, suggesting that modeling CO_2 flux can be simplified by avoiding consideration of plant functional type and management in some cases.

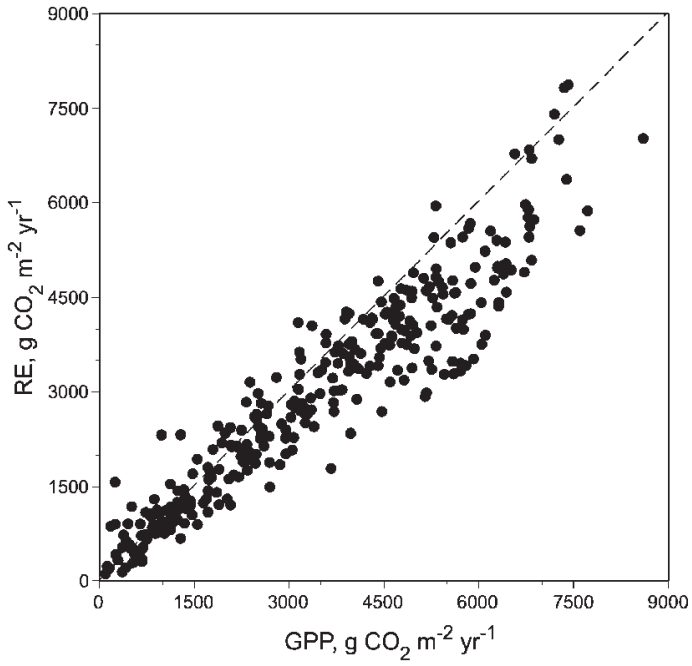

Figure 9. Scatter plot of ecosystem respiration (RE) vs. gross primary production (GPP) values for the pooled set of site-years from nonforest flux-tower stations of the world. The 1:1 diagonal is shown as a dashed line.

Gross production and ecosystem respiration of extensively managed grasslands demonstrate nonlinear patterns in response to annual precipitation that may be expressed by Mitscherlich's equation (Figs. 12A and 12B), which describes a saturated relationship (cf. Lieth 1975). Deviation of the data points from the trend, which increases in amplitude with increasing precipitation, indicates a diminishing response to precipitation. As shown in Figures 12C and 12D, the decrease of precipitation-use efficiency is linked to the dryness index (ratio of annual net radiation, R_{net}, to the amount of energy required for evaporation of precipitation, $\lambda \times$ PCPN, where λ is the latent heat coefficient; Budyko and Efimova 1968; Long et al. 1991).

IMPLICATIONS

The light-response parameters of nonforest terrestrial ecosystems have a wide range of variability, from relatively low values of photosynthetic capacity ($A_{max} = 0.2$ mg $CO_2 \cdot m^{-2} \cdot s^{-1}$ in drought-stressed grasslands), quantum yield ($\alpha = 5$ mmol $\cdot$ mol^{-1} in deserts), daytime ecosystem respiration ($r_d = 0.04$ mg $CO_2 \cdot m^{-2} \cdot s^{-1}$ in drought-stressed sagebrush steppe), and gross ecological light-use efficiency ($\varepsilon = 2.6$ mmol $\cdot$ mol^{-1} in sedge and tussock tundras of Alaska), to the highest values ever recorded for terrestrial ecosystems (inten-

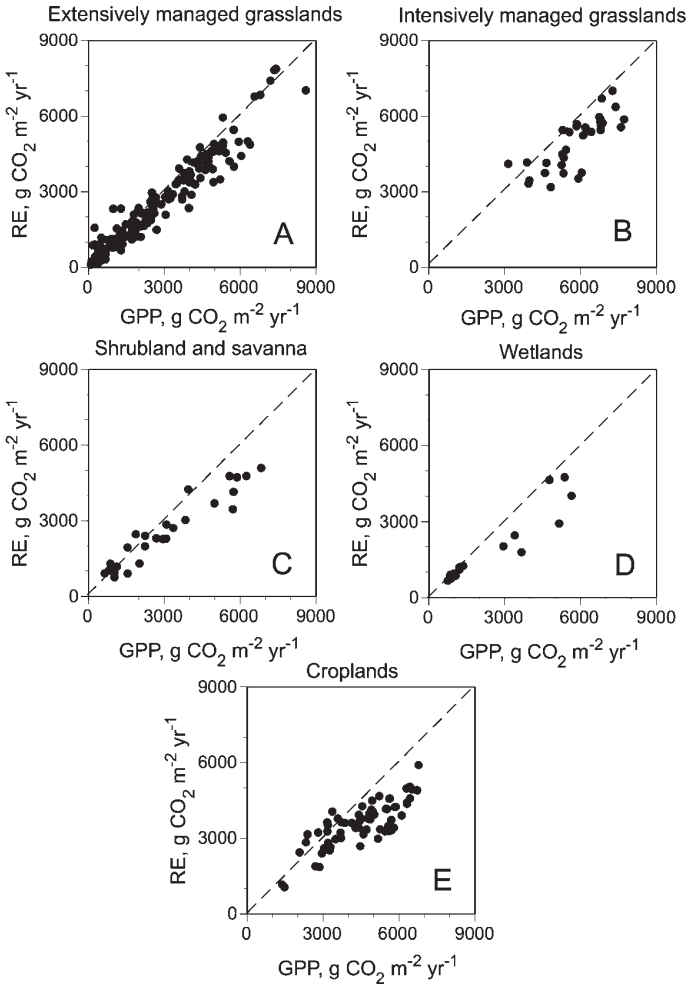

Figure 10. Scatter plots of the ecosystem respiration (RE) vs. gross primary production (GPP) values for various types of nonforest ecosystems: **A**, extensively managed grasslands; **B**, intensively managed grasslands; **C**, shrublands and savanna; **D**, wetlands; **E**, croplands.

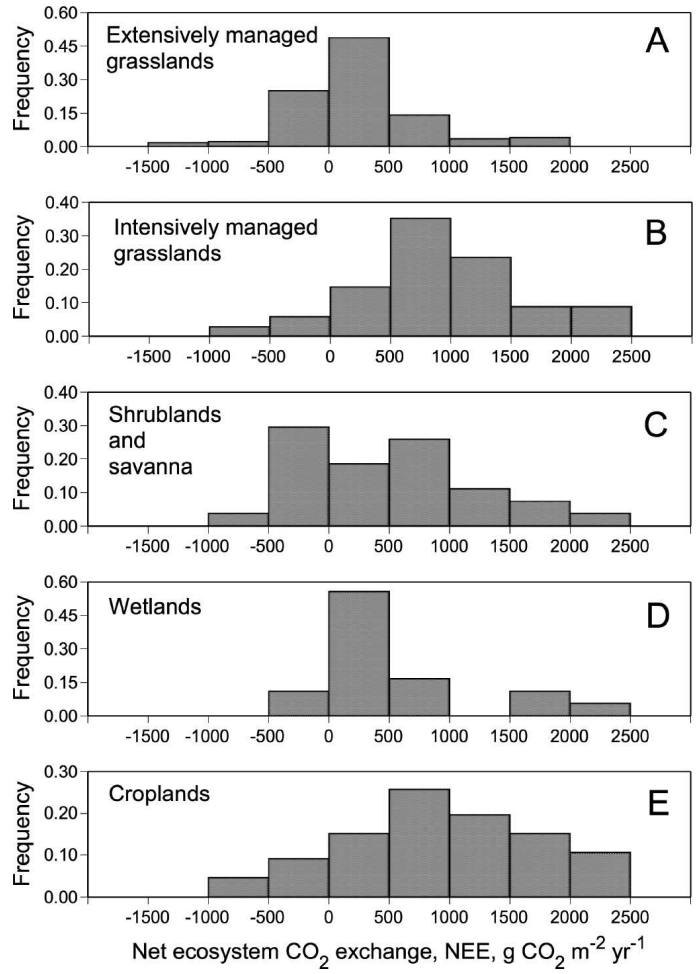

Figure 11. Histograms of statistical distributions of the annual net ecosystem CO_2 exchange values (NEE) in various types of nonforest ecosystems: **A**, extensively managed grasslands; **B**, intensively managed grasslands; **C**, shrublands and savanna; **D**, wetlands; **E**, croplands.

sively managed grasslands and agricultural crops: $A_{max} = 3.4$ mg $CO_2 \cdot m^{-2} \cdot s^{-1}$, $\alpha = 75$ mmol $\cdot$ mol^{-1}, $r_d = 0.50$ mg $CO_2 \cdot m^{-2} \cdot s^{-1}$, $\varepsilon = 59$ mmol $\cdot$ mol^{-1}). Under optimal conditions, gross primary productivity in non-forest terrestrial ecosystems can surpass productivity of forests, with maximum rates of daily gross photosynthetic assimilation, $P_{g,max}$, achieving values greater than 100 g $CO_2 \cdot m^{-2} \cdot d^{-1}$ for intensive agricultural crops ($P_{g,max} = 116$ g $CO_2 \cdot m^{-2} \cdot d^{-1}$), whereas for forest ecosystems $P_{g,max}$ values remain below 100 g $CO_2 \cdot m^{-2} \cdot d^{-1}$ (FLUXNET data base: www.fluxdata.org). Nevertheless, because of limitations by radiation, temperature, water, and nutrient resources as well as management practices, maximum values of annual GPP of nonforest ecosystems estimated from flux-tower measurements remained below 10 000 g $CO_2 \cdot m^{-2} \cdot yr^{-1}$, whereas in many types of forests they considerably exceeded this value, with maximum GPP > 14 000 calculated for a tropical forest in French Guyana (Bonal et al. 2008). The annual values of both GPP and RE for extensively and intensively managed grasslands, and shrubland/savanna ecosystems are nonlinearly associated with PCPN and dryness index, $R_{net}/(\lambda \times \text{PCPN})$, indicating the potential sensitivity of these ecosystems to anthropogenic climate change.

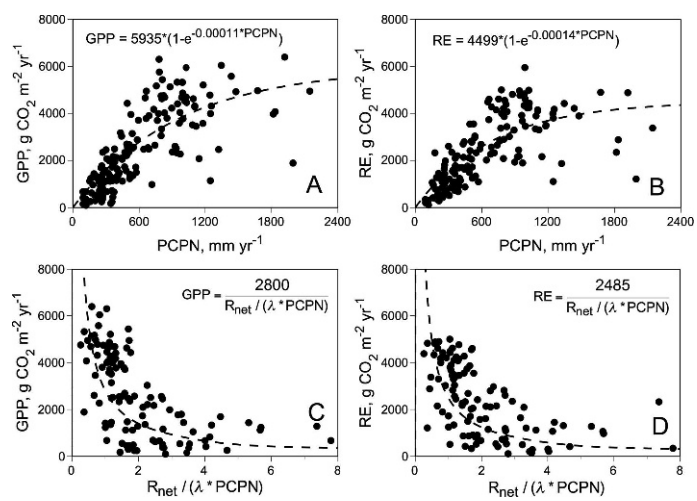

Figure 12. Response of gross primary production, GPP (**A, C**) and ecosystem respiration, RE, (**B, D**) of extensively managed grasslands on the annual precipitation, PCPN (**A, B**) and the dryness index DI = $R_{net}/(\lambda \cdot \text{PCPN})$. The dashed lines indicate nonlinear regressions describing predominant trends.

The data in our sample of 316 annual net CO_2 exchange values for nonforest ecosystems indicates that on average, nonforest ecosystems act as net biospheric sinks for atmospheric CO_2, with the highest rates of net annual CO_2 uptake occurring in agricultural crops (mean $NEE_{crop} = 933$ g $CO_2 \cdot m^{-2} \cdot yr^{-1}$) and intensively managed grasslands (mean $NEE_{grassint} = 700$ g $CO_2 \cdot m^{-2} \cdot yr^{-1}$). These data, based on continuous long-term flux-tower measurements, confirm that grasslands and agricultural crops play a significant role in the uptake of atmospheric CO_2 and its transformation to biomass and soil organic matter (cf. Lal et al. 1998; Follett et al. 2001; Follett and Schuman 2005). These findings make it necessary to reconsider conclusions of earlier authors (e.g., Smith and Falloon 2005; Conant et al. 2007 in SOCCR) concerning the negative or neutral role that agroecosystems play in carbon budgets. These earlier studies, based on C-inventory methods and usually conducted at a regional scale, did not utilize flux-tower measurements. The tower measurements analyzed in our study documented the role of many nonforest ecosystems as CO_2 sinks at the local scale. These results underscore the need to further examine the fate of carbon transported from grasslands and agroecosystems, and metabolized in and/or transported to other geographic locations. Clearly, further analyses are needed to determine the extent to which flux-tower networks and the geographic information systems and remote-sensing methods used to upscale flux measurements are representative, and to evaluate the significance of positive net CO_2 exchange for the total carbon budget of managed grasslands and intensive agricultural crops (Barcza et al. 2009).

ACKNOWLEDGMENTS

We appreciate the efforts of those who have contributed data to the US Department of Agriculture–Agricultural Research Service RANGEFLUX,[2] FLUXNET,[3] and WORLDGRASSAGRIFLUX[4] data sets: K. Akshalov,[4] V. Allard,[3,4] C. Ammann,[3] M. Aubinet,[3] M. Aurela,[3] J. Baker,[3,4] D. Baldocchi,[3] J. Balogh,[3] M. Balzarolo,[3] C. Bernacchi,[3,4] C. Bernhofer,[3] P. Béziat,[3] F. Bosveld,[3] K. Brehe,[4] N. Buchmann,[3] P. Cellier,[3] Shiping Chen,[3] R. Coulter,[3] R. Czerny,[3] E. Dellwik,[3] A. Detwiler,[4] A. J. Dolman,[3] W. Dugas,[2] M. Durikov,[4] J. Elbers,[3] W. Emmerich,[2] W. Eugster,[3,4] D. Fitzjarrald,[3] L. B. Flanagan,[3,4] J. Fuhrer,[3] T. Griffis,[3,4] M. Haferkamp,[2] R. Harding,[3] A. Hensen,[3] M. Heuer,[3,4] S. Hollinger,[3] D. Janous,[3] W. Jans,[3] T. Kato,[3] G. Katul,[3] D. Kliche,[4] W. Kutsch,[3] G. Lanigan,[3] T. Laurila,[4] P. Leahy,[3] C. Lloyd,[3] A. Lohila,[4] A. Manzi,[3] M. Marek,[3] R. Matamala,[3,4] T. Meyers,[3,4] P. Mielnick,[2] A. Miyata,[3] J. Morgan,[2] C. Moureaux,[3,4] K. A. Novick,[3] J. Olejnik,[3] J. E. Olesen,[3] W. Oechel,[3] D. Papale,[3] J. Prueger,[4] A. Raschi,[3], C. Rebmann,[3] H. da Rocha,[3] N. Rogiers,[3,4] N. Saliendra,[2] K. Schelde,[3] R.H. Skinner,[4] H. Soegaard,[3] M. Sutton,[3] A. Suyker,[3] M. Torn,[4] M. Urbaniak,[3] S. Verma,[3] M. Waterloo,[3] G. Wohlfahrt,[3,4] and B. Zhao.[3] The authors thank managers of the RANGEFLUX database Patricia Mielnick and the FLUXNET database Dario Papale, Markus Reichstein, and Deb Agarwal for assistance with updating tower flux data. We also thank Mary Brooke McEachern for help with editing the manuscript of the article. FLUXNET data used in this work are the outcome of the La Thuile FLUXNET workshop 2007, which would not have been possible without the financial support provided by CarboEuropeIP, FAO-GTOS-TCO, iLEAPS, Max Planck Institute for Biogeochemistry, National Science Foundation, University of Tuscia, and US Department of Energy. Moreover, we acknowledge databasing and technical support from Surface Energy Balance Network (SEBN, formerly GEWEX), Berkeley Water Center, Lawrence Berkeley National Laboratory, Microsoft Research eScience, Oak Ridge National Laboratory, University of California—Berkeley, and University of Virginia. The following networks participated with flux data: AmeriFlux, AfriFlux, AsiaFlux, CarboAfrica, CarboEuropeIP, ChinaFlux, Fluxnet-Canada, Ko-Flux, LBA, NECC, OzFlux, TCOS-Siberia, USCCC. AmeriFlux grant: US Department of Energy, Biological and Environmental Research, Terrestrial Carbon Program (DE-FG02-04ER63917).

LITERATURE CITED

Agarwal, D., M. Humphrey, C. van Ingen, N. Beekwilder, M. Goode, K. Jackson, M. R. L. Rodriguez, and R. Weber. 2008. FLUXNET synthesis dataset collaboration infrastructure. *FluxLetter* (*The Newsletter of FLUXNET*) 1:5–7.

Ammann, C., C. R. Flechard, J. Leifeld, A. Neftel, and J. Fuhrer. 2007. The carbon budget of newly established temperate grassland depends on management intensity. *Agriculture, Ecosystems & Environment* 121:5–20.

Anthoni, P. M., A. Freibauer, O. Kolle, and E. D. Schulze. 2004. Winter wheat carbon exchange in Thuringia, Germany. *Agricultural and Forest Meteorology* 121:55–67.

Aubinet, M., A. Grelle, A. Ibrom, Ü. Rannik, J. Moncrieff, T. Foken, A. S. Kowalski, P. H. Martin, P. Berbigier, C. Bernhofer, R. Clement, J. Elbers, A. Granier, T. Grünwald, K. Morgenstern, K. Pilegaard, C. Rebmann, W. Snijders, R. Valentini, and T. Vesala. 2000. Estimates of the annual net carbon and water exchange of forests: the EUROFLUX methodology. *Advances in Ecological Research* 30:113–175.

Aubinet, M., C. Moureaux, B. Bodson, D. Dufranne, B. Heinesch, M. Suleau, F. Vancutsem, and A. Vilret. 2009. Carbon sequestration by a crop over a 4-year sugar beet/winter wheat/seed potato/winter wheat rotation cycle. *Agricultural and Forest Meteorology* 149:407–418.

Austin, R. B., G. Kingston, P. C. Longden, and P. A. Donovan. 1978. Gross energy yields and the support energy requirements for the production of sugar from beet and cane: a study of four production areas. *Journal of Agricultural Science* 91:661–675.

Baker, J. M., and T. J. Griffis. 2005. Examining strategies to improve the carbon balance of corn/bean agriculture using eddy covariance and mass balance techniques. *Agricultural and Forest Meteorology* 128:163–177.

Baldocchi, D. 2008a. Advanced topics in biometeorology and micrometeorology. Available at: http://nature.berkeley.edu/biometlab/espm228/. Accessed 30 November 2009.

Baldocchi, D. 2008b. "Breathing" of the terrestrial biosphere: lessons learned from a global network of carbon dioxide flux measurement systems. *Australian Journal of Botany* 56:1–26.

Baldocchi, D., E. Falge, L. Gu, R. J. Olson, D. Hollinger, S. Running, P. Anthoni, C. Bernhofer, K. Davis, R. Evans, J. Fuentes, A. Goldstein, G. Katul, B. Law, X. Lee, Y. Malhi, T. Meyers, W. Munger, W. Oechel, K. T. Paw U, K. Pilegaard, H. P. Schmid, R. Valentini, S. Verma, T. Vesala, K. Wilson, and S. Wofsy. 2001. FLUXNET: a new tool to study the temporal and spatial variability of ecosystem-scale carbon dioxide, water vapor, and energy flux densities. *Bulletin of the American Meteorological Society* 82: 2415–2434.

Baldocchi, D., and L. Xu. 2005. Carbon exchange of deciduous broadleaved forests in temperate and Mediterranean regions. *In:* H. Griffiths and P. G. Jarvis [eds.]. The carbon balance of forests. New York, NY, USA: Taylor and Francis. p. 187–215.

Barcza, Z., L. Haszpra, H. Kondo, N. Saigusa, S. Yamamoto, and J. Bartholy. 2003. Carbon exchange of grass in Hungary. *Tellus B* 55:187–196.

Barcza, Z., A. Kern, L. Haszpra, and N. Kljun. 2009. Spatial representativeness of tall eddy covariance measurements using remote sensing and footprint analysis. *Agricultural and Forest Meteorology* 149:795–807.

Bernacchi, C. J., S. E. Hollinger, and T. Meyers. 2006. Corrigendum: the conversion of the corn/soybean ecosystem to no-till agriculture may result in a carbon sink. *Global Change Biology* 12:1585–1586.

Béziat, P., E. Ceschia, and G. Dedieu. 2009. Carbon balance of a three crop succession over two cropland sites in South-West France. *Agricultural and Forest Meteorology* 149:1628–1645.

Birdsey, R. A., J. C. Jenkins, M. Johnston, E. Huber-Sannwald, B. Amero, B. de Jong, J. D. E. Barra, N. R. French, F. Garcia-Oliva, M. Harmon, L. S. Heath, V. J. Jaramillo, K. Johnsen, B. E. Law, E. Martin-Spiotta, O. Masera, R. Neilson, Y. Pan, and K. S. Pregitzer. 2007. North American forests. *In:* A. W. King, L. Dilling, G. P. Zimmerman, D. M. Fairman, R. A. Houghton, G. Marland, A. Z. Rose, and T. J. Wilbanks [eds.]. The first state of the carbon cycle report (SOCCR): The North American carbon budget and implications for the global carbon cycle. A report by the U.S. Climate Change Science Program and the Subcommittee on Global Change Research. Asheville, NC, USA: National Oceanic and Atmospheric Administration, National Climatic Data Center. p. 117–126.

Blackman, F. F. 1905. Optima and limiting factors. *Annals of Botany* 19:281–295.

Bonal, D., A. Bosc, J. Y. Goret, B. Burban, P. Gross, J. M. Bonnefond, J. Elbers, S. Ponton, D. Epron, J. M. Guehl, and A. Granier. 2008. The impact of severe dry season on net ecosystem exchange in the Neotropical rainforest of French Guiana. *Global Change Biology* 14:1917–1933.

Boyer, J. S. 1982. Plant productivity and environment. *Science* 218:443–448.

Bridgham, S. D., J. P. Megonigal, J. K. Keller, N. B. Bliss, and C. Trettin. 2007. Wetlands. *In*: A. W. King, L. Dilling, G. P. Zimmerman, D. M. Fairman, R. A. Houghton, G. Marland, A. Z. Rose, and T. J. Wilbanks [eds.]. The first state of the carbon cycle report (SOCCR): the North American carbon budget and implications for the global carbon cycle. A report by the U.S. Climate Change Science Program and the Subcommittee on Global Change Research. Asheville, NC, USA: National Oceanic and Atmospheric Administration, National Climatic Data Center. p. 117–126.

Budyko, M. I., and N. A. Efimova. 1968. The use of solar energy by the natural plant cover of the USSR. *Botanicheskii Zhurnal* 53:1384–1389.

Burba, G., and D. Anderson. 2007. Introduction to the eddy covariance method. General guidelines, and conventional workflow. LI-COR Biosciences. Available at: http://www.licor.com/env/PDF_Files/EddyCovariance_readonly.pdf. Accessed 30 November 2009.

Buyanovsky, G. A., and G. H. Wagner. 1998. Changing role of cultivated land in the global carbon cycle. *Biology and Fertility of Soils* 27:242–245.

CarbonTracker. 2009. Available at: http://www.esrl.noaa.gov/gmd/ccgg/carbontracker/. Accessed 30 November 2009.

Ciais, P., P. Friedlingstein, A. Friend, and D. S. Schimel. 2001. Integrating global models of terrestrial primary productivity. *In:* J. Roy, B. Saugier, and H. A. Mooney [eds.]. Terrestrial global productivity. San Diego, CA, USA: Academic Press. p. 449–478.

Colinvaux, P. A. 1993. Ecology 2. New York, NY, USA: Wiley. 688 p.

Conant, R. T., K. Paustian, F. Garcia-Oliva, H. H. Janzen, M. J. Jaramillo, D. E. Johnson, and S. N. Kulshreshtha. 2007. Agricultural and grazing lands. *In:* A. W. King, L. Dilling, G. P. Zimmerman, D. M. Fairman, R. A. Houghton, G. Marland, A. Z. Rose, and T. J. Wilbanks [eds.]. The first state of the carbon cycle report (SOCCR): The North American carbon budget and implications for the global carbon cycle. A report by the U.S. Climate Change Science Program and the Subcommittee on Global Change Research. Asheville, NC, USA: National Oceanic and Atmospheric Administration, National Climatic Data Center. p. 107–116.

Cooper, J. P. 1970. Potential production and energy conversion in temperate and tropical grasses. *Herbage Abstracts* 40:1–13.

Cramer, W., R. J. Olson, S. D. Prince, and J. M. O. Scurlock and members of the Global Primary Production Data Initiative. 2001. Determining present patterns of global productivity. *In:* J. Roy, B. Saugier, and H. A. Mooney [eds.]. Terrestrial global productivity. San Diego, CA, USA: Academic Press. p. 429–448.

Davidson, E. A., and I. A. Janssens. 2006. Temperature sensitivity of soil carbon decomposition and feedbacks to climate change. *Nature* 440:165–173.

Denmead, O. T., and R. H. Shaw. 1962. Availability of soil water to plants as affected by soil moisture content and meteorological conditions. *Agronomy Journal* 54:385–390.

Dugas, W. A., M. L. Heuer, and H. S. Mayeux. 1999. Carbon dioxide fluxes over bermudagrass, native prairie, and sorghum. *Agricultural and Forest Meteorology* 93:121–139.

Eastin, J. D., and C. Y. Sullivan. 1984. Environmental stress influences on plant persistence, physiology, and production. *In:* M. B. Tesar [ed.]. Physiological basis of crop growth and development. Madison, WI, USA: American Society of Agronomy and Crop Science Society of America. p. 201–236.

Emmerich, W. E. 2003. Carbon dioxide fluxes in a semiarid environment with high carbonate soils. *Agricultural and Forest Meteorology* 116:91–102.

Falge, E., J. Tenhunen, D. Baldocchi, M. Aubinet, P. Bakwin, P. Berbigier, C. Bernhofer, J. M. Bonnefond, G. Burba, R. Clement, K. J. Davis, J. A. Elbers, M. Falk, A. H. Goldstein, A. Grelle, A. Granier, T. Grünwald, J. Gudmundsson, D. Hollinger, I. A. Janssens, P. Keronen, A. S. Kowalski, G. Katul, B. E. Law, Y. Malhi, T. Meyers, R. K. Monson, E. Moors, J. W. Munger, W. Oechel, K. T. P. U. K. Pilegaard, U. Rannik, C. Rebmann, A. Suyker, H. Thorgeirsson, G. Tirone, A. Turnipseed, K. Wilson, and S. Wofsy. 2002. Phase and amplitude of ecosystem carbon release and uptake potentials as derived from FLUXNET measurements. *Agricultural and Forest Meteorology* 113:75–95.

Farrell, A. E., M. O'Hare, D. M. Kammen, R. J. Plevin, B. T. Turner, and A. D. Jones. 2006. Ethanol can contribute to energy and environmental goals. *Science* 311:506–508.

Follett, R. F., J. M. Kimble, and R. Lal [eds.]. 2001. The potential of U.S. grazing lands to sequester carbon and mitigate the greenhouse effect. Boca Raton, FL, USA: Lewis Publishers. 442 p.

Follett, R. F., and G. E. Schuman. 2005. Grazing land contributions to carbon sequestration. *In:* D. A. McGilloway [ed.]. Grassland: a global resource. Wageningen, the Netherlands: Wageningen Academic Publishers. p. 265–277.

Frank, A. B., P. L. Sims, J. A. Bradford, P. C. Mielnick, W. A. Dugas, and H. S. Mayeux. 2001. Carbon dioxide fluxes over three Great Plains grasslands. *In:* R. F. Follett, J. M. Kimble, and R. Lal [eds.]. The potential of U.S. grazing lands to sequester carbon and mitigate the greenhouse effect. Boca Raton, FL, USA: Lewis Publishers. p. 167–187.

Funk, J. L., and M. T. Lerdau. 2004. Photosynthesis in forest canopies. *In:* M. D. Lowman and H. B. Rinker [eds.]. Forest canopies. Amsterdam, the Netherlands: Elsevier Academic Press. p. 335–358.

Gilmanov, T. G., A. B. Frank, M. R. Haferkamp, T. P. Meyers, J. A. Morgan, L. L. Tieszen, B. K. Wylie, and L. B. Flanagan. 2005. Integration of CO_2 flux and remotely-sensed data for primary production and ecosystem respiration analyses in the Northern Great Plains: potential for quantitative spatial extrapolation. *Global Ecology and Biogeography* 14:271–292.

Gilmanov, T. G., D. A. Johnson, and N. Z. Saliendra. 2003a. Growing season CO_2 fluxes in a sagebrush-steppe ecosystem in Idaho: Bowen ratio/energy balance measurements and modeling. *Basic and Applied Ecology* 4:167–183.

Gilmanov, T. G., D. A. Johnson, N. Z. Saliendra, K. Akshalov, and B. K. Wylie. 2004. Gross primary productivity of the true steppe in Central Asia in relation to NDVI: scaling-up CO_2 fluxes. *Environmental Management* 39:S492–S508.

Gilmanov, T. G., J. F. Soussana, L. Aires, V. Allard, C. Ammann, M. Balzarolo, Z. Barcza, C. Bernhofer, C. L. Campbell, A. Cernusca, A. Cescatti, J. Clifton-Brown, B. O. M. Dirks, S. Dore, W. Eugster, J. Fuhrer, C. Gimeno, T. Gruenwald, L. Haszpra, A. Hensen, A. Ibrom, A. F. G. Jacobs, M. B. Jones, G. Lanigan, T. Laurila, A. Lohila, G. Manca, B. Marcolla, Z. Nagy, K. Pilegaard, K. Pinter, C. Pio, A. Raschi, N. Rogiers, M. J. Sanz, P. Stefani, M. Sutton, Z. Tuba, R. Valentini, M. L. Williams, and G. Wohlfahrt. 2007. Partitioning European grassland net ecosystem CO_2 exchange into gross primary productivity and ecosystem respiration using light response function analysis. *Agriculture, Ecosystems and Environment* 121:93–120.

Gilmanov, T. G., T. J. Svejcar, D. A. Johnson, R. F. Angell, N. Z. Saliendra, and B. K. Wylie. 2006. Long-term dynamics of production, respiration, and net CO_2 exchange in two sagebrush-steppe ecosystems. *Rangeland Ecology and Management* 59:585–599.

Gilmanov, T. G., S. B. Verma, P. L. Sims, T. P. Meyers, J. A. Bradford, G. G. Burba, and A. E. Suyker. 2003b. Gross primary production and light response parameters of four Southern Plains ecosystems estimated using long-term CO_2-flux tower measurements. *Global Biogeochemical Cycles* 17, doi: 10.1029/2002GB002023.

Gilmanov, T. G., and WORLDGRASSAGRIFLUX Data Set Participants. 2007. Productivity, respiration, CO_2 sink potential, and light-response parameters of world grasslands derived from flux-tower data partitioning. *Eos, Transactions, American Geophysical Union, Fall Meeting Supplement* 88(52):Abstract B32B-03.

Good, N. E., and D. H. Bell. 1980. Photosynthesis, plant productivity and crop yield. *In:* P. S. Carlson [ed.]. The biology of crop productivity. New York, NY, USA: Academic Press. p. 3–51.

Goulden, M. L., J. W. Munger, S. M. Fan, B. C. Daube, and S. C. Wofsy. 1996. Measurements of carbon sequestration by long-term eddy covariance: methods and critical evaluation of accuracy. *Global Change Biology* 2:169–182.

Griffiths, H., and P. Jarvis [eds.]. 2005. The carbon balance of forest biomes. New York, NY, USA: Taylor & Francis.

Hendricks, D. M. D., J. van Huissteden, A. J. Dolman, and M. K. van der Molen. 2007. The full greenhouse gas balance of an abandoned peat meadow. *Biogeosciences* 4:414–424.

Jacobs, C. M. J., A. F. G. Jacobs, F. C. Bosveld, D. M. D. Hendriks, A. Hensen, P. S. Kroon, E. J. Moors, L. Nol, A. Schrier-Uijl, and E. M. Veenendaal. 2007. Variability of annual CO_2 exchange from Dutch grasslands. *Biogeosciences Discussions* 4:1499–1534.

Jaksic, V., G. Kiely, J. Albertson, R. Oren, G. Katul, P. Leahy, and K. A. Byrne. 2006. Net ecosystem exchange of grassland in contrasting wet and dry years. *Agricultural and Forest Meteorology* 139:323–334.

Jarvis, P. G. 1994. Capture of carbon dioxide by a coniferous forest. *In:* J. L. Monteith, R. K. Scott, and M. H. Unsworth [eds.]. Resource capture by crops. Loughborough, Leicestershire, United Kingdom: Nottingham University Press. p. 351–374.

King, A. W., L. Dilling, G. P. Zimmerman, D. M. Fairman, R. A. Houghton, G. Marland, A. Z. Rose, and T. J. Wilbanks [eds.]. 2007. The first state of the carbon cycle report (SOCCR): the North American carbon budget and implications for the global carbon cycle. A report by the U.S. Climate Change Science Program and the Subcommittee on Global Change Research. Asheville, NC, USA: National Oceanic and Atmospheric Administration, National Climatic Data Center. 240 p.

Körner, C. 2003. Slow in, rapid out—carbon flux studies and Kyoto target. *Science* 300:1242–1243.

Lal, R., J. M. Kimble, R. F. Follett, and C. V. Cole [eds.]. 1998. The potential of U.S. cropland to sequester carbon and mitigate the greenhouse effect. Chelsea, MI, USA: Ann Arbor Press. 128 p.

Larcher, W. W. 1995. Physiological plant ecology: ecophysiology and stress physiology of functional groups. Berlin, Germany: Springer-Verlag. 506 p.

Le Houèrou, H. N., and C. H. Hoste. 1977. Rangeland production and annual rainfall relations in the Mediterranean basin and in the African Sahelo-Sudanian Zone. *Journal of Range Management* 30:181–189.

Lee, X., W. Massman, and B. Law [eds.]. 2004. Handbook of micrometeorology: a guide for surface flux measurement and analysis. Dordrecht, the Netherlands: Kluwer Academic Publishers. 250 p.

Lieth, H. 1975. Modeling the primary productivity of the world. *In:* H. Lieth and R. H. Whittaker [eds.]. Primary productivity of the biosphere. New York, NY, USA: Springer-Verlag. p. 237–263.

Loehle Enterprises. 2007. Global optimization 6.0. Global nonlinear optimization using Mathematica. Naperville, IL, USA: Loehle Enterprises.

Long, S. P., M. B. Jones, and M. J. Roberts [eds.]. 1991. Primary productivity of grass ecosystems of the tropics and sub-tropics. London, United Kingdom: Chapman & Hall. 267 p.

Meyers, T. P. 2001. A comparison of summertime water and CO_2 fluxes over rangeland for well watered and drought conditions. *Agricultural and Forest Meteorology* 106:205–214.

Mielnick, P. C., and W. A. Dugas. 2000. Soil CO_2 flux in a tallgrass prairie. *Soil Biology and Biochemistry* 32:221–228.

Mielnick, P. C., W. A. Dugas, H. B. Johnson, H. W. Polley, and J. Sanabria. 2001. Net grassland carbon flux over a subambient to superambient CO_2 gradient. *Global Change Biology* 7:747–754.

Mitscherlich, E. A. 1909. Das Gesetz des Minimums und das Gesetz des abnehmenden Bodenertrages. *Landwirtschaftliches Jahrbuch der Schweiz* 38:537–552.

Moffat, A. M., D. Y. Hollinger, A. D. Richardson, A. G. Barr, C. Beckstein, B. H. Braswell, G. Churkina, A. R. Desai, E. Falge, J. H. Gove, M. Heimann, D. Hui, A. J. Jarvis, J. Kattge, A. Noormets, V. J. Stauch, D. Papale, and M. Reichstein. 2007. Comprehensive comparison of gap-filling techniques for eddy covariance net carbon fluxes. *Agricultural and Forest Meteorology* 147:209–232.

Monteith, J. L. 1972. Solar radiation and productivity in tropical ecosystems. *Journal of Applied Ecology* 9:747–766.

Mordacq, L., J. Ghasghaie, and B. Saugier. 1991. A simple method for measuring the gas exchange of small trees. *Functional Ecology* 5:572–576.

Moureaux, C., A. Debacq, B. Bodson, B. Heinesch, and M. Aubinet. 2006. Annual net ecosystem carbon exchange by a sugar beet crop. *Agricultural and Forest Meteorology* 139:25–39.

Novick, K. A., M. B. S. Siqueira, J. Juang, R. Oren, P. C. Stoy, G. G. Katul, and D. S. Ellsworth. 2004. Carbon dioxide and water vapor exchange in a warm temperate grassland. *Oecologia* 138:259–274.

Odum, E. P. 1959. Fundamentals of ecology. Philadelphia, PA, USA: Saunders. 384 p.

Odum, H. T. 1956. Primary production in flowing waters. *Limnology and Oceanography* 1:102–117.

Olson, J. S., J. A. Watts, and L. J. Allison. 1983. Carbon in live vegetation of major world ecosystems. Washington, DC, USA: US Department of Energy, Oak Ridge National Laboratory Technical Report ORNL-5862. 152 p.

Owen, K. E., E. Falge, R. Geyer, X. Xiao, P. Stoy, C. Ammann, A. Arain, M. Aubinet, M. Aurela, C. Bernhofer, B. H. Chojnicki, A. Granier, T. Gruenwald, J. Hadley, B. Heinesch, D. Hollinger, A. Knohl, W. Kutsch, A. Lohila, T. Meyers, E. Moors, C. Moureaux, K. Pilegaard, N. Saigusa, S. Verma, T. Vesala, C. Vogel, J. Tenhunen, M. Reichstein, and Q. Wang. 2007. Linking flux network measurements to continental scale simulations: ecosystem carbon dioxide exchange capacity under non-water-stressed conditions. *Global Change Biology* 13:734–760.

Patzek, T. W., J. Lee, B. Li, J. Padnick, S. A. Yee, S. M. Anti, R. Campos, and K. W. Ha. 2005. Ethanol from corn: clean renewable fuel for the future, or drain on our resources and pockets? *Environment, Development and Sustainability* 7:319–336.

Peters, W., A. R. Jacobson, C. Sweeney, A. E. Andrews, T. J. Conway, K. Masarie, J. B. Miller, L. M. P. Bruhwiler, G. Pétron, A. I. Hirsch, D. E. J. Worthy, G. R. van der Werf, J. T. Randerson, P. O. Wennberg, M. Krol, and P. P. Tans. 2007. An atmospheric perspective on North American carbon dioxide exchange: CarbonTracker. *Proceedings of the National Academy of Sciences of the United States of America* 104:18925–18930.

Powlson, D. S., A. B. Riche, and I. Shield. 2005. Biofuels and other approaches for decreasing fossil fuel emissions from agriculture. *Annals of Applied Biology* 146:193–201.

Rabinowich, E. I. 1951. Photosynthesis and related processes. New York, NY, USA: Interscience Publishers. 1208 p.

Reichstein, M., E. Falge, D. Baldocchi, D. Papale, R. Valentini, M. Aubinet, P. Berbigier, C. Bernhofer, N. Buchmann, M. Falk, T. Gilmanov, A. Granier, T. Grünwald, K. Havránková, D. Janous, A. Knohl, T. Laurela, A. Lohila, D. Loustau, G. Matteucci, T. Meyers, F. Miglietta, J. M. Ourcival, D. Perrin, J. Pumpanen, S. Rambal, E. Rotenberg, M. Sanz, J. Tenhunen, G. Seufert, F. Vaccari, T. Vesala, and D. Yakir. 2005. On the separation of net ecosystem exchange into assimilation and ecosystem respiration: review and improved algorithm. *Global Change Biology* 11:1424–1439.

Reicosky, D. C. 1997. Tillage-induced CO_2 emission from soil. *Nutrient Cycling in Agroecosystems* 49:273–285.

Rodin, L. E., and N. I. Bazilevich. 1968. Production and mineral cycling in terrestrial vegetation. Edinburgh, Scotland: Oliver and Boyd. 288 p.

Rosenzweig, M. L. 1968. Net primary production of terrestrial communities: prediction from climatological data. *American Naturalist* 102:67–74.

Ruimy, A., P. G. Jarvis, and D. D. Baldocchi. 1995. CO_2 fluxes over plant canopies and solar radiation: a review. *Advances in Ecological Research* 26:1–68.

Sala, O. E., W. J. Parton, L. A. Joyce, and W. K. Lauenroth. 1988. Primary production of the central grassland region of the United States. *Ecology* 69:40–45.

Singh, J. S., M. J. Trlica, P. G. Risser, R. E. Redmann, and J. K. Marshall. 1980. Autotrophic subsystem. *In:* A. I. Breymeyer and G. M. Van Dyne [eds.]. Grasslands, systems analysis and man. Cambridge, United Kingdom: Cambridge University Press. p. 59–200.

Skinner, R. H., M. S. Corson, and T. G. Gilmanov. 2008. Simulating pasture photosynthesis and respiration. *Agronomy Journal* 100:801–807.

Slatyer, R. O. 1967. Plant–water relationships. New York, NY, USA: Academic Press. 366 p.

Smith, P., and P. Falloon. 2005. Carbon sequestration in European croplands. *In:* H. Griffiths and P. G. Jarvis [eds.]. The carbon balance of forest biomes. New York, NY, USA: Taylor and Francis. p. 47–55.

Soussana, J. F., V. Allard, K. Pilegaard, P. Ambus, C. Amman, C. Campbell, E. Ceschia, J. Clifton-Brown, S. Czobel, R. Domingues, C. Flechard, J. Fuhrer, A. Hensen, L. Horvath, M. Jones, G. Kasper, C. Martin, Z. Nagy, A. Neftel, A. Raschi, S. Baronti, R. M. Rees, U. Skiba, P. Stefani, G. Manca, M. Sutton, Z. Tubaf, and R. Valentini. 2007. Full accounting of the greenhouse gas (CO_2, N_2O, CH_4) budget of nine European grassland sites. Agriculture, Ecosystems and Environment. *The Greenhouse Gas Balance of Grasslands in Europe* 121:121–134.

Stoy, P. C., J. Y. Juang, K. A. Novick, J. M. Uebelherr, R. Oren, G. G. Katul, and M. B. S. Siqueira. 2006. An evaluation of models for partitioning eddy covariance-measured net ecosystem exchange into photosynthesis and respiration. *Agricultural and Forest Meteorology* 141:2–18.

Suyker, A. E., S. B. Verma, and B. G. G. 2003. Interannual variability in net CO_2 exchange of a native tallgrass prairie. *Global Change Biology* 9:255–265.

Svejcar, T., R. Angell, J. Bradford, W. Dugas, W. Emmerich, A. Frank, T. Gilmanov, M. Haferkamp, D. Johnson, H. Mayeux, P. Mielnick, J. Morgan, N. Saliendra, G. Schuman, P. Sims, and K. Snyder. 2008. Carbon fluxes on North American rangelands. *Rangeland Ecology and Management* 61:465–474.

Svejcar, T., H. Mayeux, and R. Angell. 1997. The rangeland carbon dioxide flux project. *Rangelands* 19:16–18.

Tamiya, H. 1951. Some theoretical notes on the kinetics of algal growth. *Botanical Magazine* 6:167–173.

Tarnocai, C., C. L. Ping, and J. Kimble. 2007. Carbon cycle in the permafrost region of North America. *In:* A. W. King, L. Dilling, G. P. Zimmerman, D. M. Fairman, R. A. Houghton, G. Marland, A. Z. Rose, and T. J. Wilbanks [eds.]. The first state of the carbon cycle report (SOCCR): The North American carbon budget and implications for the global carbon cycle. A report by the U.S. Climate Change Science Program and the Subcommittee on Global Change Research. Asheville, NC, USA: National Oceanic and Atmospheric Administration, National Climatic Data Center. p. 127–138..

Thornley, J. H. M., and I. R. Johnson. 2000. Plant and crop modelling. A mathematical approach to plant and crop physiology. Caldwell, NJ, USA: The Blackburn Press. 669 p.

Verma, S. B., A. Dobermann, K. G. Cassman, D. T. Walters, J. M. Knops, T. J. Arkebauer, A. E. Suyker, G. G. Burba, B. Amos, H. Yang, D. Ginting, K. G. Hubbard, A. A. Gitelson, and E. A. Walter-Shea. 2005. Annual carbon dioxide exchange in irrigated and rainfed maize-based agroecosystems. *Agricultural and Forest Meteorology* 131:77–96.

Walter, H. 1939. Grassland, Savanne und Busch der ariden Teile Afrikas in ihrer ökologische Bedingtheit. *Jahrbuch fur wissenschaftliche Botanik* 87:850–860.

Weaver, J. E. 1924. Plant production as a measure of environments. *Journal of Ecology* 12:205–237.

Whittaker, R. H., and G. E. Likens. 1973. Carbon in the biota. *In:* G. M. Woodwell and E. V. Pecan [eds.]. Carbon and the biosphere. Springfield, VA, USA: National Technical Information Service. p. 281–302.

Wildung, R. E., T. R. Garland, and R. L. Buschbom. 1975. The interdependent effects of soil temperature and water content on soil respiration rate and plant root decomposition in arid grassland soils. *Soil Biology and Biochemistry* 7:373–378.

Wohlfahrt, G., C. Newesely, A. Cernusca, M. Bahn, and A. Haslwanter. 2005. Estimation of daytime ecosystem respiration to determine gross primary production of a mountain meadow. *Agricultural and Forest Meteorology* 130:13–25.

Wolfram Research. 2009. Wolfram Mathematica 7. Complete Documentation. Available at: http://reference.wolfram.com/mathematica/guide/Mathematica.html. Accessed 30 November 2009.

Woodward, F. I., M. R. Lomas, and S. E. Lee. 2001. Predicting the future productivity and distribution of global terrestrial vegetation. *In:* J. Roy, B. Saugier, and H. A. Mooney [eds.]. Terrestrial global productivity. San Diego, CA, USA: Academic Press. p. 521–541.

Xu, L., and D. D. Baldocchi. 2004. Seasonal variation in carbon dioxide exchange over a Mediterranean annual grassland in California. *Agricultural and Forest Meteorology* 123:79–96.

Yuan, W., G. Zhou, L. L. Tieszen, D. Baldocchi, C. Bernhofer, H. Gholz, A. H. Goldstein, M. L. Goulden, D. Y. Hollinger, Y. Hu, B. E. Law, P. C. Stoy, T. Vesala, S. C. Wofsy, and S. Liu. 2007. Deriving a light use efficiency model from eddy covariance flux data for predicting daily gross primary production across biomes. *Agricultural and Forest Meteorology* 143:189–207.

Zhang, L., E. Fosnight, L. L. Tieszen, L. Ji, T. Gilmanov, B. Wylie, and T. Loveland. 2007. Evaluation and comparison of gross primary production estimates for the Northern Great Plains grasslands. *Remote Sensing of Environment* 106:173–189.

Zhang, L. M., Y. Gui-Rui, X. M. Sun, X. F. Wen, C. Y. Ren, Y. L. Fu, Q. K. Li, Z. Q. Li, Y. F. Liu, D. X. Guan, and J. H. Yan. 2006. Seasonal variation of ecosystem apparent quantum yield (α) and maximum photosynthesis rate (P_{max}) of different forest ecosystems in China. *Agricultural and Forest Meteorology* 137:176–187.

Zhao, L., S. Gu, G. Yu, X. Zhao, Y. Li, S. Xu, and H. Zhou. 2006. Diurnal, seasonal and annual variation in net ecosystem CO_2 exchange of an alpine shrubland on Qinghai-Tibetan plateau. *Global Change Biology* 12:1940–1953.

APPENDIX: LIST OF SYMBOLS

Latin Symbols

A_{max} = maximum gross photosynthetic assimilation (mg $CO_2 \cdot m^{-2} \cdot s^{-1}$)

F_c = net CO_2 flux (mg $CO_2 \cdot m^{-2} \cdot s^{-1}$; g $CO_2 \cdot m^{-2} \cdot d^{-1}$)

GPP = annual gross primary production (g $CO_2 \cdot m^{-2} \cdot yr^{-1}$)

IntNEE = integrated net ecosystem CO_2 exchange (g $CO_2 \cdot m^{-2}$)

k_T = coefficient in the exponential equation for respiration temperature dependence $(^\circ C)^{-1}$

L = leaf area index ($m^2 \cdot m^{-2}$)

L_{max} = seasonal maximum leaf area index ($m^2 \cdot m^{-2}$)

P_d = daytime integral of the net ecosystem CO_2 flux (g $CO_2 \cdot m^{-2} \cdot d^{-1}$)

P_g = gross photosynthetic assimilation (mg $CO_2 \cdot m^{-2} \cdot s^{-1}$; g $CO_2 \cdot m^{-2} \cdot d^{-1}$)

Q = incoming photosynthetically active radiation (μmol quanta $\cdot m^{-2} \cdot s^{-1}$; mol quanta $\cdot m^{-2} \cdot d^{-1}$)

Q_a = absorbed photosynthetically active radiation (μmol quanta $\cdot m^{-2} \cdot s^{-1}$; mol quanta $\cdot m^{-2} \cdot d^{-1}$)

PCPN = atmospheric precipitation ($mm \cdot d^{-1}$, $mm \cdot yr^{-1}$)

r_d = daytime ecosystem respiration rate (mg $CO_2 \cdot m^{-2} \cdot s^{-1}$)

R_d = daytime ecosystem respiration (mg $CO_2 \cdot m^{-2} \cdot s^{-1}$; g $CO_2 \cdot m^{-2} \cdot d^{-1}$)

R_e = total ecosystem respiration (mg $CO_2 \cdot m^{-2}\ s^{-1}$; g $CO_2 \cdot m^{-2} \cdot d^{-1}$)

RE = annual total ecosystem respiration (g $CO_2 \cdot m^{-2} \cdot yr^{-1}$)

RH = air relative humidity (%)

R_n = nighttime ecosystem respiration (mg $CO_2 \cdot m^{-2} \cdot s^{-1}$; g $CO_2 \cdot m^{-2} \cdot d^{-1}$)

R_{net} = net radiation ($W \cdot m^{-2}$; $MJ \cdot m^{-2} \cdot d^{-1}$)

r_0 = ecosystem respiration rate at temperature $T_s = 0^\circ C$ (mg $CO_2 \cdot m^{-2} \cdot s^{-1}$)

r_n = nighttime ecosystem respiration rate (mg $CO_2 \cdot m^{-2} \cdot s^{-1}$)
R_n = nighttime ecosystem respiration (mg $CO_2 \cdot m^{-2} \cdot s^{-1}$; g $CO_2 \cdot m^{-2} \cdot d^{-1}$)
R_{net} = net radiation ($W \cdot m^{-2}$; $MJ \cdot m^{-2} \cdot d^{-1}$)
T_a = air temperature (°C)
t_r = time of sunrise (h)
t_s = time of sunset (h)
T_s = soil temperature (typically, at 5-cm depth; °C)
T_{year} = mean annual temperature (°C)
$V_{c,max}$ = maximum rate of carboxylation (mg CO_2 $m^{-2} \cdot s^{-1}$)
VPD = vapor pressure deficit (kPa)
W_s = volumetric soil moisture ($m^3 \cdot m^{-3}$)

Greek Symbols

α = apparent quantum yield of gross photosynthetic assimilation (mmol $CO_2 \cdot$ mol quanta^{-1})
ε, ε_{ecol} = gross ecological light-use efficiency (mmol $CO_2 \cdot$ [mol incident quanta]$^{-1}$)
ε_{phys} = gross physiological light-use efficiency (mmol $CO_2 \cdot$ [mol absorbed quanta]$^{-1}$)
λ = latent heat of evaporation ($MJ \cdot kg^{-1}$)
θ = convexity (curvature) coefficient of the light-response equation (dimensionless)
ρ_d = diffusive resistance to CO_2 transport ($s \cdot m^{-1}$)
ρ_x = carboxylation resistance to carbon transport ($s \cdot m^{-1}$)